

**The author(s) shown below used Federal funding provided by the U.S. Department of Justice to prepare the following resource:**

**Document Title:** Novel Blood Protein Modification Assay for Retrospective Detection of Drug Exposure

**Author(s):** Anthony P. DeCaprio, Ph.D.

**Document Number:** 252918

**Date Received:** May 2019

**Award Number:** 2015-NE-BX-K001

**This resource has not been published by the U.S. Department of Justice. This resource is being made publically available through the Office of Justice Programs' National Criminal Justice Reference Service.**

**Opinions or points of view expressed are those of the author(s) and do not necessarily reflect the official position or policies of the U.S. Department of Justice.**

**Agency:** National Institute of Justice, Office of Justice Programs

**Award Number:** 2015-NE-BX-K001

**Project Title:** Novel Blood Protein Modification Assay for Retrospective Detection of Drug Exposure

**PI:** Anthony P. DeCaprio, Ph.D.  
Associate Professor  
Department of Chemistry & Biochemistry  
Florida International University  
305-348-2195  
adecapr@fiu.edu

**Submitting Official:** Mr. Roberto M. Gutierrez  
Assistant Vice President for Research  
Office of Research and Economic Development  
Florida International University  
11200 SW 8<sup>th</sup> St., MARC 430  
Miami, FL 33199  
305-348-2494  
gutierr@fiu.edu

**Submission Date:** October 9, 2018

**DUNS:** 0712988140000

**EIN:** 65-0177616

**Recipient Organization:**

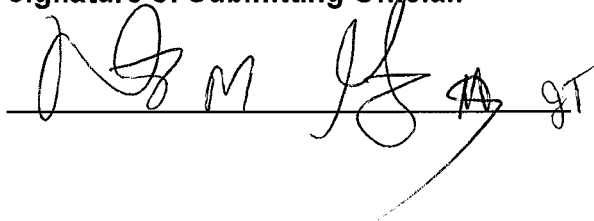
The Florida International University Board of Trustees  
11200 SW 8<sup>th</sup> St., MARC 430  
Miami, FL 33199

**Award Period:** 1/1/2016 - 9/30/18

**Report Period End Date:** 9/30/18

**Progress Report:** Semi-annual Report #6 (part 2 Cumulative Final)

**Signature of Submitting Official:**

A handwritten signature in black ink, appearing to read 'R M Gutierrez', is written over a horizontal line. The signature is stylized and includes a large flourish at the end.

## **Purpose**

Detection and confirmation of human exposure to drugs typically relies on measurement of parent compounds or specific metabolites in blood, urine, or an alternative sample matrix. This “biomonitoring” approach is widely employed for forensic toxicological applications and has been standardized for many xenobiotics. Despite its broad acceptance, biomonitoring does have significant drawbacks with regard to the useful time frame for drug detection. Most drugs and their metabolites (with the exception of lipophilic drugs) are cleared within a week, after which they can no longer be directly detected in these sample matrices. As a result, blood or urine measurements alone generally cannot provide data on past episodic exposure, cumulative exposure, or time-dependent exposure profiles for drugs. Nevertheless, such data may be critically important in forensic toxicology, for example as evidence in drug facilitated crimes and for measurement of drug compliance or abstinence in pain drug management, addiction rehabilitation programs, and probation/parole criminal justice situations.

Currently, retrospective biomonitoring of drug use or exposure is limited to analysis of hair, for which numerous methods and a large literature database exist. While clearly useful for this purpose, hair analysis does have some technical and interpretive challenges. Another potential technology for longer-term monitoring of drug exposure involves measurement of the products of covalent modification of free thiol moieties of blood proteins, such as hemoglobin (Hb) and serum albumin (SA), by reactive metabolites (RM) of drugs. Since they typically persist for the life of the protein, such protein “adducts” can provide a much longer window of detection of exposure than is generally possible by direct measurement of parent compound or a metabolite.

While widely used in human exposure assessment for environmental and occupational chemicals, applications of protein adducts as markers of illicit drug exposure are virtually nonexistent. Regardless, preliminary studies in this laboratory has demonstrated *in vitro* modification of glutathione (GSH) and model thiol-containing peptides by RM of certain abused drugs, suggesting the potential feasibility of this approach.

### **Project Design and Methods**

Task 1 of this project consisted of development and optimization of an *in vitro* assay system to generate RM of 16 selected drugs and assessment of the *in vitro* adduction potential of drug RM with thiol containing trapping agents (GSH and a model thiol-containing peptide). These drugs included alprazolam (ALP), buprenorphine (BUP), cocaine (COC), diazepam (DZP), methadone (META), methamphetamine (METH), methylenedioxymethamphetamine (MDMA), methylenedioxypyrovalerone (MDPV), methylone (METY), morphine (MOR), naltrexone NAL), oxycodone (OXY),  $\alpha$ -pyrrolidinopentiophenone ( $\alpha$ -PVP),  $\Delta^9$ -tetrahydrocannabinol (THC), acetaminophen (APAP) and clozapine (CLZ). Task 2 of the project included detection and confirmation of thiol modifications of human Hb by RM of selected drugs following *in vitro* incubation in the same assay system.

Relevant data for all experiments are provided in the Appendix to this summary report.

***In vitro generation of RM and thiol trapping assay:*** An *in vitro* metabolic system was developed to facilitate drug conversion to RM and adduction to GSH, an N-terminal

acetylated cysteine-containing peptide (Ac-PAACAA) model peptide, and a model protein (human Hb). For GSH studies, final concentrations of assay components were: 1 mM test drug, 1 mg/mL Human liver microsomes (HLM), 2 mM NADPH, 3 mM MgCl<sub>2</sub>, 3 mM glucose-6-phosphate (G6P), 0.4 units/mL glucose-6-phosphate dehydrogenase (G6PD), 2 mM GSH, in 50 mM sodium phosphate buffer, pH 7.4. In the optimized assay, drugs were added to plastic vials and residual solvent removed via vacufuge. Remaining components (except GSH) were added to provide the above listed final concentrations. Contents were vortexed and pre-incubated for 15 min at 37°C. Following pre-incubation, GSH was added and the vial was vortexed again briefly and then incubated at 37°C for 3 h. Once incubation was complete, vials were centrifuged at 15,000 x g at 4°C for 30 min. A 100 µL aliquot was removed from the vial and added to a clean LC-MS vial for MS analysis.

For model protein studies, a modified *in vitro* assay was developed that involved the analysis of tryptic peptides of adducted protein. This assay consisted of the same mixture as above but containing 5 mg/mL Hb in 25 mM ammonium bicarbonate buffer, pH 7.6. The mixture was incubated at 37°C for 3 h and centrifuged for 30 min at 100,000 x g. After centrifugation, a freshly-prepared 15 mM solution of iodoacetamide was added and the mixture incubated at RT in the dark for 1 h. Adducted Hb was then extracted from the reaction mixture using a 3K Da cutoff spin filter, followed by addition of 0.25 mg/mL of trypsin and incubation at 37°C overnight.

**Mass Spectrometric Identification of GSH, peptide, and protein adducts:** GSH adduct analysis in negative ESI mode was performed on an Agilent 6460 LC-QqQ-MS with mobile phases (A) water with 0.1% acetic acid; and (B) 95% acetonitrile, 4.9%

water with 0.1% acetic acid. For GSH adducts, precursor ion scans using a product ion  $m/z$  of 272, a characteristic transition for GSH and GSH-containing compounds, were performed. The mass window was set to  $m/z$  400-800, in order to avoid unnecessary interference from non-adducted GSH. From the total ion chromatogram, an extracted ion chromatogram was collected for each of the significant peaks, and a corresponding structure was proposed for each ion detected. Following initial GSH adduct analysis by negative mode LC-QqQ-MS, adduct peak masses were analyzed using negative mode targeted scanning on an Agilent 6530 LC-QTOF-MS (HRMS). HRMS analysis was performed at collision energies of 10, 20, and 40 eV so that transitions could be observed at a level which would maximize their count and determine distinguishing values. Peaks observed by both LC-QqQ-MS and LC-QTOF-MS were considered as confirmed adduct peaks.

Adduct structures were proposed based on accurate mass data for the molecular ion of each drug-GSH adduct and for major MS/MS fragments. For novel adducts, a list of metabolites potentially formed *in situ* was compiled using published metabolism data as available and, where not available, using *in silico* metabolite prediction methods. Structures associated with more than one metabolic transformation were also considered. The final theoretical adduct list therefore consisted of multiple target structures for each drug. Calculated molecular ion masses of the theoretical adduct structures were then compared to those observed in the HRMS analysis for each drug to identify tentative positive hits.

For model peptide studies, assay supernatant was collected and analyzed using an Agilent Model 6460 QqQ MS. Peptides were analyzed by direct flow injection analysis (FIA) with no LC column separation and MS was conducted in positive ionization mode.

The FIA approach allowed for the concurrent detection of all possible components present in the sample, including the parent drug, metabolites, and peptide adducts.

For Hb peptide digests, chromatographic separation utilized an Agilent Zorbax Rapid Resolution HD Eclipse Plus C18 column with gradient elution. HRMS analysis of tryptic peptides utilized positive ESI full scan mode with an Agilent 1290 Infinity UHPLC coupled to the Agilent 6460 MS.

## **Data Analysis and Results**

***Drug-GSH Adduct Studies:*** Using the initial QqQ-MS screening approach, a total of 20 potentially significant GSH adduction products were identified for 10 of the 16 drugs examined, including APAP, CLZ, COC, DZP, MDMA, MDPV, MOR, NAL, OXY, and THC. Multiple adduct structures were also observed for a number of drugs. In contrast, GSH adducts were not observed for ALP, BUP, DZP, META, MET, and METY under these screening conditions. Target products detected by low resolution MS were then further examined using high resolution LC-QTOF-MS/MS analysis (HRMS).

HRMS analysis confirmed the positive results indicated the screening assay. A total of 22 individual adduct structures were identified by HRMS for the 10 drugs yielding positive results. Ten of these have been previously reported in the literature, while 12 are novel entities not previously reported, including those for DZP, NAL, OXY, and THC. The structures reported previously all have masses which matched closely with those observed in spectra collected in the present study. The reason(s) for the lack of observed GSH adduction with the other five drugs are unclear at the present time, but may involve unfavorable reaction conditions or insufficient analytical sensitivity due to ionization issues or other factors. These issues are being explored in continuing

studies.

*In silico* metabolite prediction analysis suggested that, in many cases, formation of an adduct was associated with an 'NIH shift' pathway. There are several proposed mechanisms by which an NIH shift may occur, however, the prevailing theory, which has been experimentally corroborated, involves formation of an unstable epoxide which then undergoes a hydride shift. Plausible structures were proposed for the majority of the previously unreported adducts identified in the present study, based upon HRMS accurate mass and MS/MS data and likely metabolic transformations.

GSH adducts of THC have not previously been reported in the literature. The present study identified four species consistent with covalent adduction of GSH with THC, all proposed to result from modification of THC metabolites oxidized at the 11 position or on the pentyl chain of the parent drug. The proposed structures for two adducts are consistent with adducts formed from the stable metabolites 11-OH- $\Delta^9$ -THC and 11-nor-9-carboxy- $\Delta^9$ -THC, with direct binding to GSH. Additional data are required to identify the exact nature of the metabolic modifications present in the other two THC adducts and the location of the C-S linkage in each species.

***Drug-Model Peptide Adduct Studies:*** Evidence for covalent adduction to the model Cys peptide was obtained for 14 of the 16 tested drugs, with data for 11 drugs confirmed by MS/MS analysis. For these drugs, parent ions, metabolites, and their transitions could be observed. The appearance of new peaks whose masses correspond to the adduct products were determined. The MS/MS fragmentation of the adducted peptide peaks indicated that they corresponded to the drug-peptide adductions. Of the drugs tested, only META and THC did not show detectable



formation of peptide adducts. In particular, OXY, ALP, METY, and MOR showed a high potential for peptide adduct formation. Several potential adducts at lower  $m/z$ , possibly corresponding to adducts formed by ALZ metabolites, were also noted. In contrast, METY and MOR clearly yielded only single adduct ions corresponding to addition of one parent drug molecule. The adducted peptide parent ions corresponded primarily to the major adduct detected for each drug. However, for a number of drugs, several minor adducts were also noted. DZP, MDPV,  $\alpha$ -PVP, and COC also formed adducts, although these were in lower abundance than the other drugs with positive results. Control experiments, conducted in the absence of HLM and/or NADPH, did not result in adduct formation, confirming that formation of RM is required for adduction to occur.

Studies were also performed to assess the effect of increasing drug concentration on the amount of acetylated peptide remaining and the amount of adducted peptide formed during the metabolic assay. In these studies, decreasing concentrations of METH and NAL were evaluated. Even at drug concentrations as low as 10  $\mu$ M, the formation of the corresponding adducts was observed. These results suggest the likelihood of covalent thiol adduction by these drugs at physiological levels.

**Drug-Protein Adduct Studies:** Studies were conducted to determine whether RM of the selected drugs can covalently adduct free thiols in human hemoglobin (Hb). For this purpose, purified Hb was incubated in the *in vitro* trapping assay as described above, followed by trypsin proteolysis and HRMS peptide analysis. The initial LC-QTOF-MS data analyzed with BioConfirm produced positive results for the adduction of APAP, confirming via MS data what has been reported previously in the literature regarding pharmacological and HPLC studies. APAP adduction was observed for both Hb  $\beta^{93}$ Cys

and the less reactive Hb  $\beta^{112}\text{Cys}$ . Adduction was also observed for  $\alpha\text{-PVP}$ , METH, NAL, OXY, and THC, producing a total of 11 potential adducts. The adducted drug species mass observed for THC corresponded to the mass of the 11-hydroxy-THC metabolite adducted to Hb, also in agreement with the major THC adduct observed in the GSH studies. METH exhibited adducts at both the  $\beta^{93}\text{Cys}$  and  $\alpha^{104}\text{Cys}$  residues, while THC modified only the  $\beta^{93}\text{Cys}$ . BioConfirm also successfully identified MS/MS fragmentation at high mass accuracy for two of the adducts; APAP-modified Hb  $\beta^{93}\text{Cys}$  and  $\alpha\text{-PVP}$ -modified Hb  $\beta^{93}\text{Cys}$ . These data confirm the Hb binding potential of a number of the drugs tested to date. This work is continuing in additional studies for the remaining selected drugs.

### **Major Findings**

- *In vitro* metabolic assays for generation of RM of 16 selected drugs, and for adduct trapping with GSH, a thiol-containing model peptide, and human Hb were developed and optimized.
- Of the 16 drugs tested for GSH adduction potential, APAP, CLZ, COC, DZP, MDMA, MDPV, MOR, NAL, OXY, and THC demonstrated GSH adduction potential, with a total of 22 individual GSH adducts identified. Ten of these have been previously reported in the literature, while 12 are novel entities not previously reported, including those for DZP, NAL, OXY, and THC.
- Evidence for adduction of the thiol-containing model peptide was obtained for 14 of the 16 tested drugs, with data for 11 drugs confirmed by MS/MS analysis. For these drugs, parent ions, metabolites, and their transitions could be observed. Of the drugs

tested, only META and THC did not show detectable formation of peptide adducts.

- *In vitro* studies with APAP, METH, THC, a-PVP, OXY, and NAL indicated that all of these drugs are capable of covalent binding to reactive Cys thiols in human Hb.
- In summary, proof of principle has been obtained that all of the drugs tested have the potential to form RM capable of covalently modifying GSH, thiol-containing peptides, and/or human Hb. This represents a key step towards developing a useful drug monitoring strategy based on blood protein modification that will allow the project to progress to the next stage involving development and validation of a practical assay.

### **Implications for Criminal Justice Policy and Practice in the United States**

The major purpose of this study was to generate basic research data and preliminary applied data to support an ultimate goal of developing protein adduct based biomarker assays for compounds of forensic interest, including drugs of abuse. Such tools would allow for exposure assessment for these compounds over a much longer period of time than is currently possible and provide an alternative or complement to hair analysis. A longer window of detection for drugs of abuse is critically important in forensic toxicology, such as in drug facilitated sexual assault cases and for measurement of drug compliance or abstinence in pain drug management, rehabilitation programs, and probation/parole criminal justice situations. Consequently, this novel approach is anticipated to significantly benefit forensic science for criminal justice research by providing additional tools for detecting and quantifying important agents of forensic interest in biological specimens over longer periods of time.

# **Appendix**

## **Final Summary Overview**

**Award Number 2015-NE-BX-K001**

### **Novel Blood Protein Modification Assay for Retrospective Detection of Drug Exposure**

**Table 1:** Data for parent drugs tested for GSH adduction potential.

Drug	Formula	Exact Mass (Da)
Acetaminophen (APAP)	C <sub>8</sub> H <sub>9</sub> NO <sub>2</sub>	151.063
Alprazolam (ALP)	C <sub>17</sub> H <sub>13</sub> ClN <sub>4</sub>	308.083
Buprenorphine (BUP)	C <sub>29</sub> H <sub>41</sub> NO <sub>4</sub>	467.304
Clozapine (CLZ)	C <sub>18</sub> H <sub>19</sub> ClN <sub>4</sub>	326.130
Cocaine (COC)	C <sub>17</sub> H <sub>21</sub> NO <sub>4</sub>	303.147
Diazepam (DZP)	C <sub>16</sub> H <sub>13</sub> ClN <sub>2</sub> O	284.072
Methadone (META)	C <sub>21</sub> H <sub>27</sub> NO	309.209
Methamphetamine (METH)	C <sub>10</sub> H <sub>15</sub> N	149.120
Methylenedioxymethamphetamine (MDMA)	C <sub>11</sub> H <sub>15</sub> NO <sub>2</sub>	193.110
Methylenedioxypyrovalerone (MDPV)	C <sub>16</sub> H <sub>21</sub> NO <sub>3</sub>	275.152
Methylone (METY)	C <sub>11</sub> H <sub>13</sub> NO <sub>3</sub>	207.090
Morphine (MOR)	C <sub>17</sub> H <sub>19</sub> NO	285.137
Naltrexone (NAL)	C <sub>20</sub> H <sub>23</sub> NO <sub>4</sub>	341.163
Oxycodone (OXY)	C <sub>18</sub> H <sub>21</sub> NO <sub>4</sub>	315.147
α-Pyrrolidinopentiophenone (α-PVP)	C <sub>15</sub> H <sub>21</sub> NO	231.162
Δ <sup>9</sup> -Tetrahydrocannabinol (THC)	C <sub>21</sub> H <sub>30</sub> O <sub>2</sub>	314.225

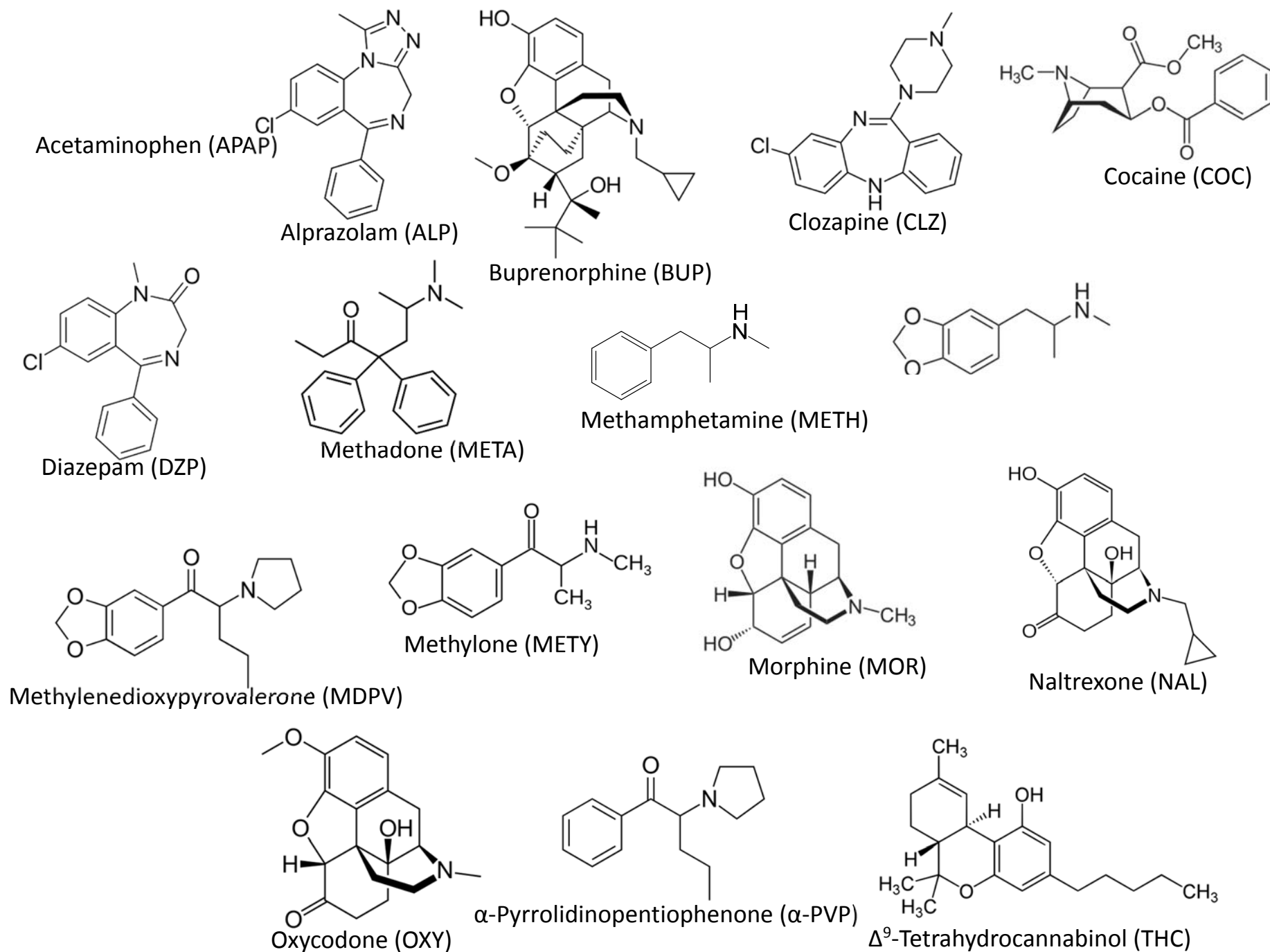


**Figure 1:** Structures for all 16 of the drugs of interest in this study. Each drug is labelled with its abbreviation as outlined in Table 1.

This document was prepared by the author(s) using Federal funds provided by the U.S. Department of Justice. Opinions or points of view expressed are those of the author(s) and do not necessarily reflect the official position or policies of the U.S. Department of Justice.

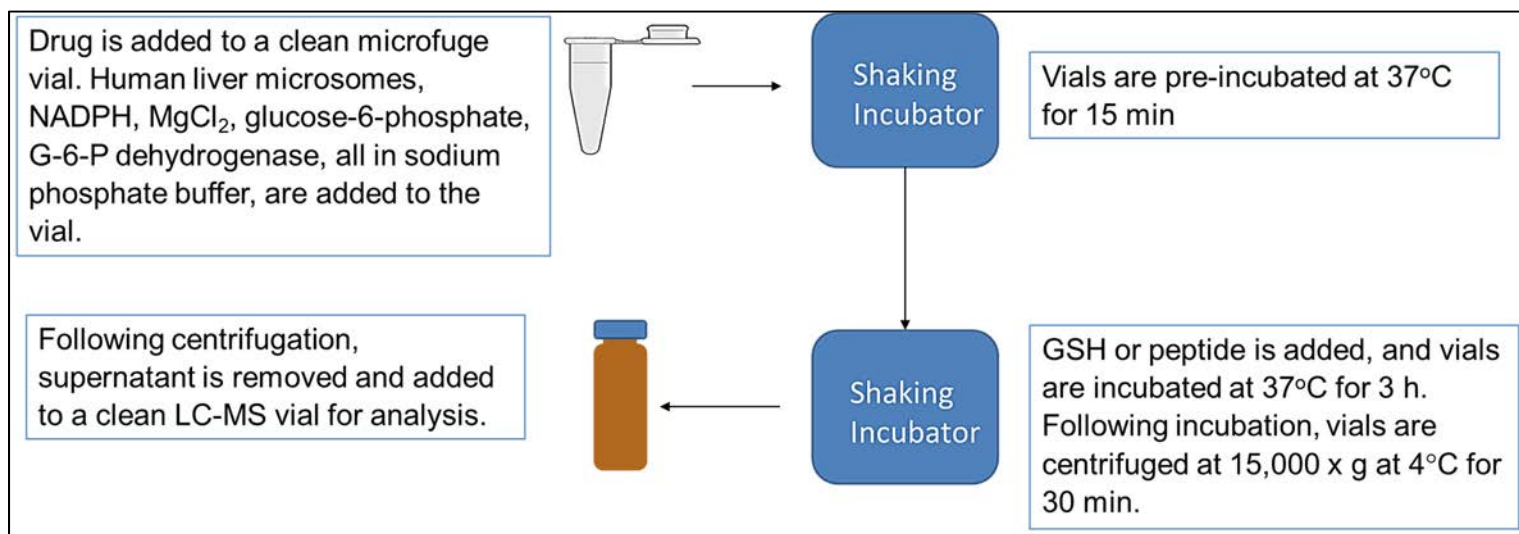


**Figure 2:** Details of *in vitro* drug metabolism/trapping assay used for GSH and model peptide adduction studies.

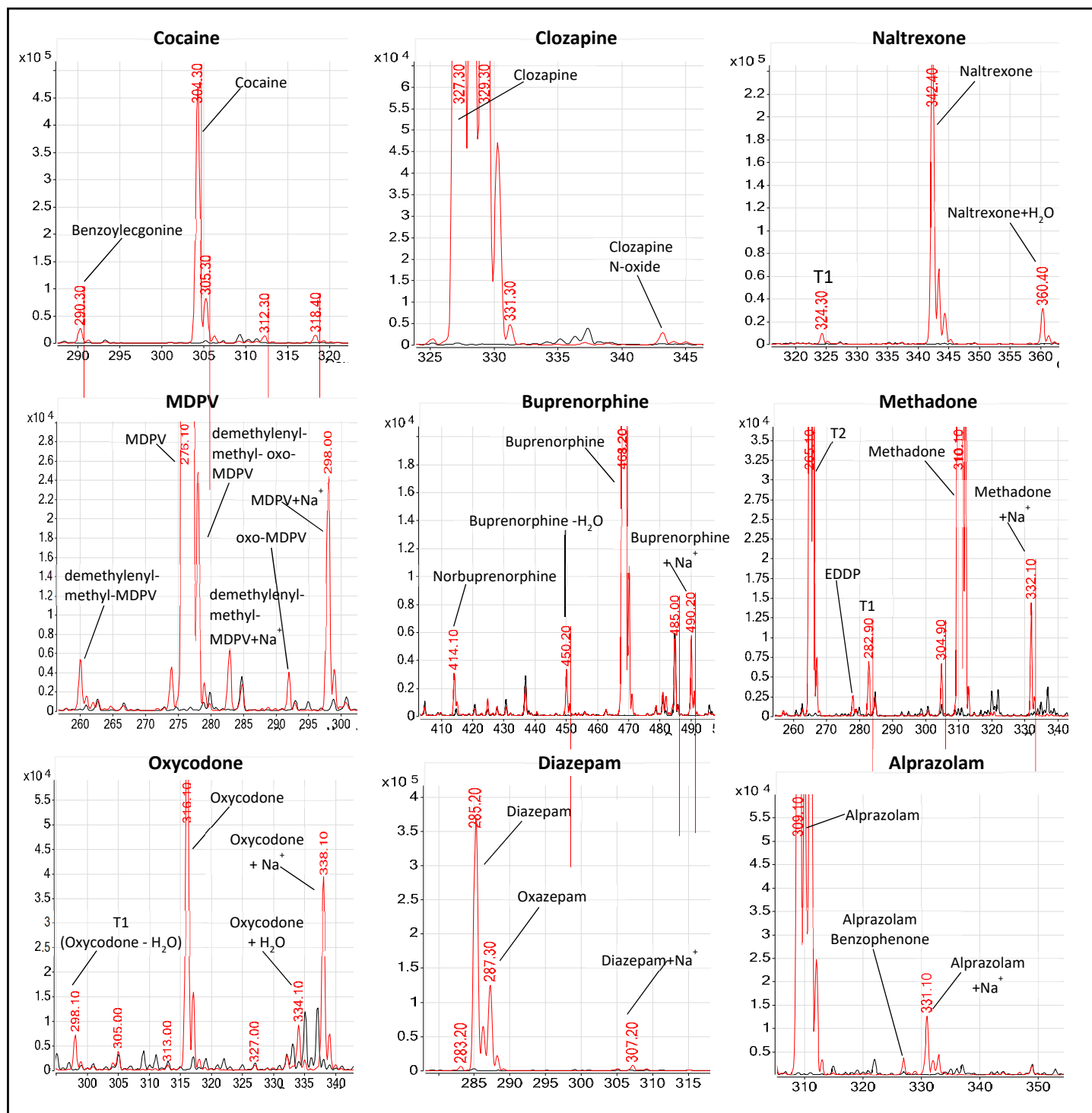


**Figure 3:** LC-QqQ-MS/MS spectra for parent drugs and metabolites identified in *in vitro* assays (red). Control spectra (no drug) shown in black.



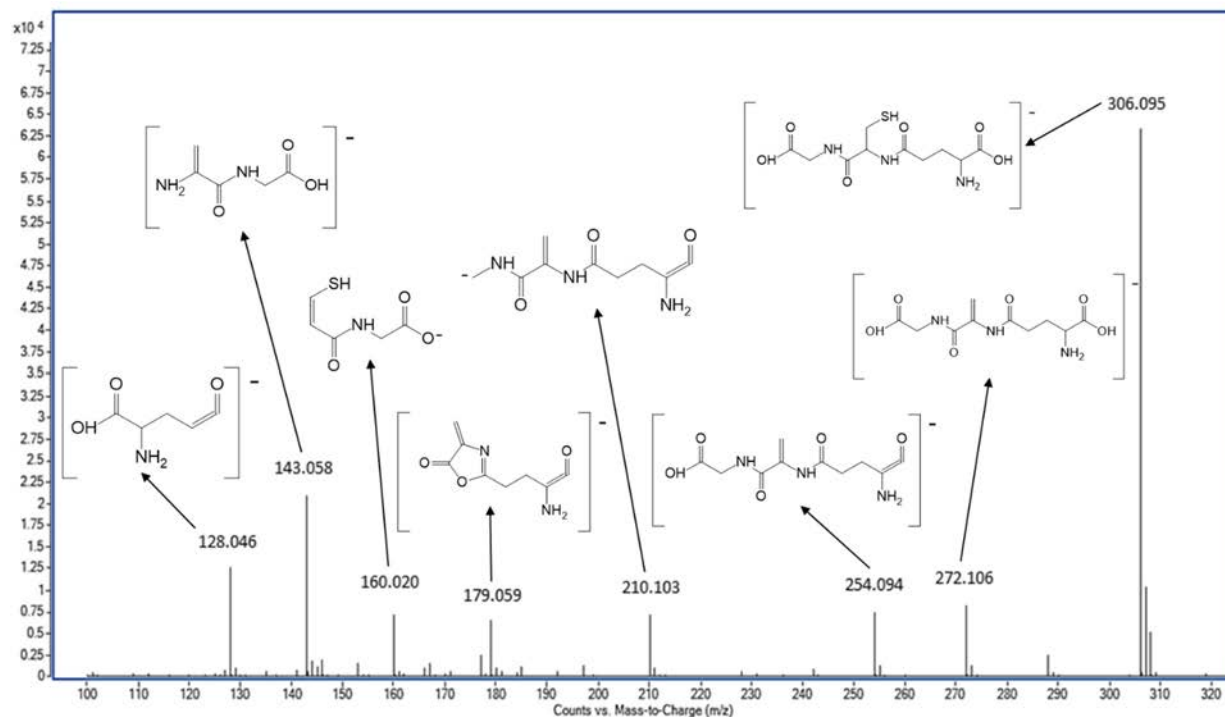


**Figure 4:** LC-QTOF-MS/MS data collected for glutathione. Labelled peaks correspond to a known characteristic GSH ion. Negative ionization structures for each peak are provided for each peak.

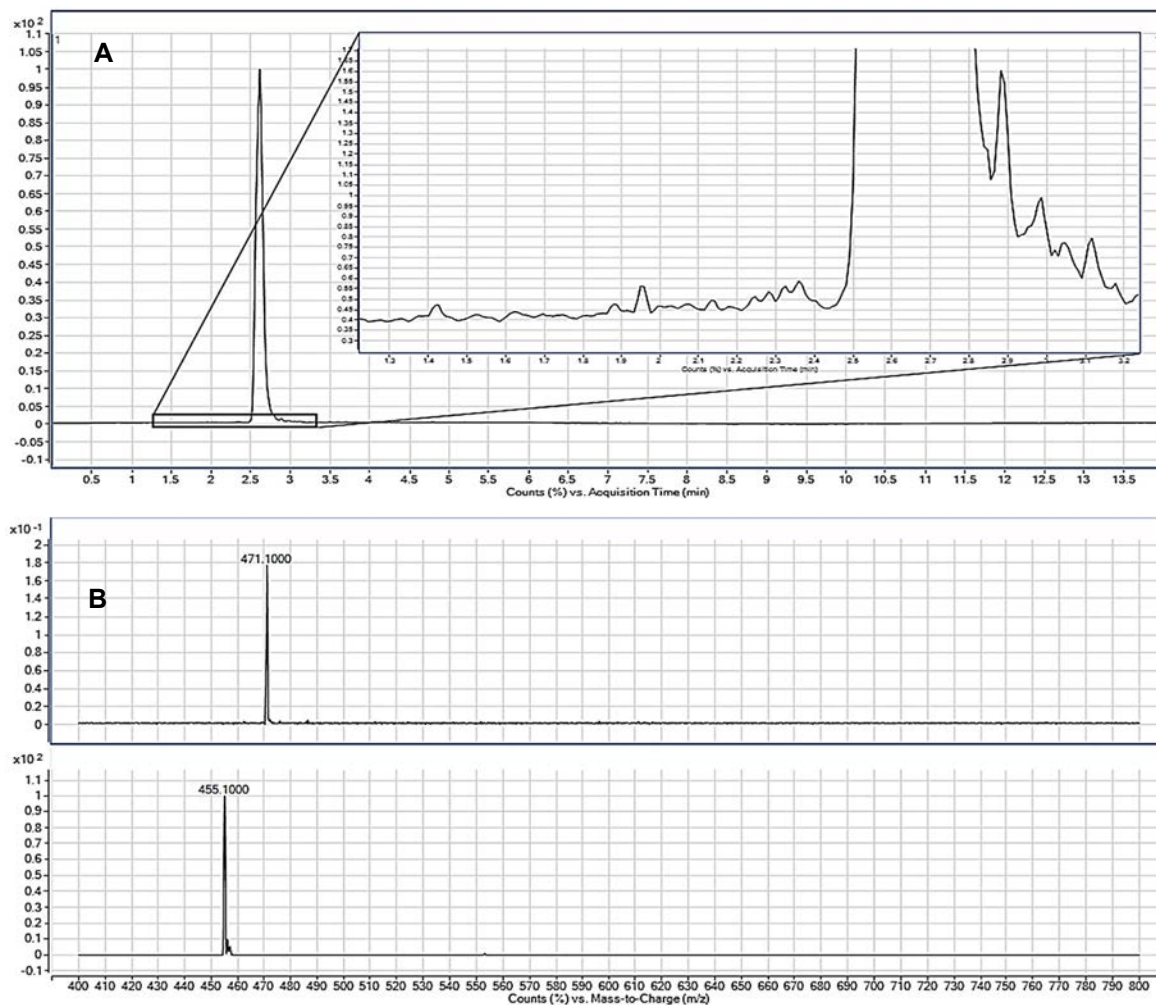


**Figure 5:** (A) TIC of APAP+GSH collected by product ion scan mode via LC-QqQ-MS in negative ionization mode. Inset is zoomed-in portion around the base of the major peak, showing multiple peaks with lesser intensities. (B) XICs for ions at  $m/z$  471 and 455, the two relevant peaks of interest from the TIC.

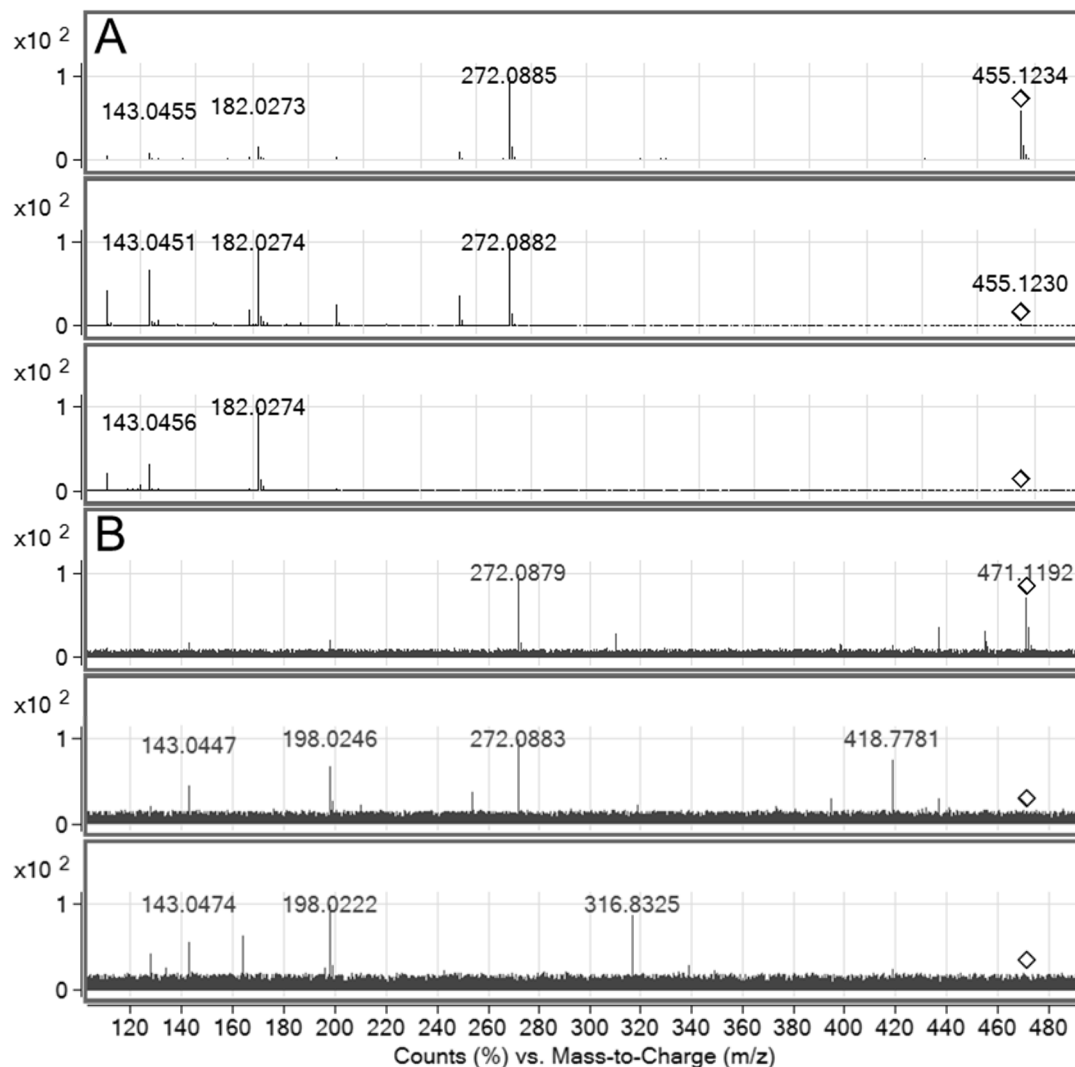


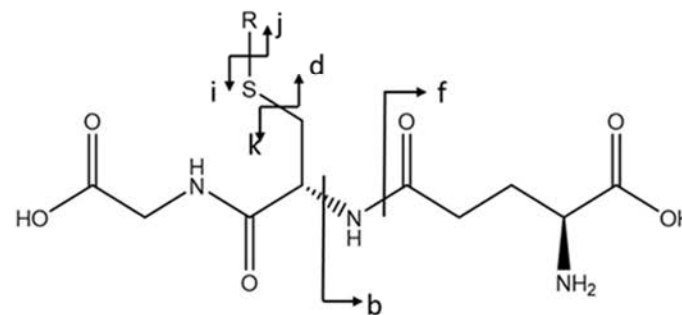
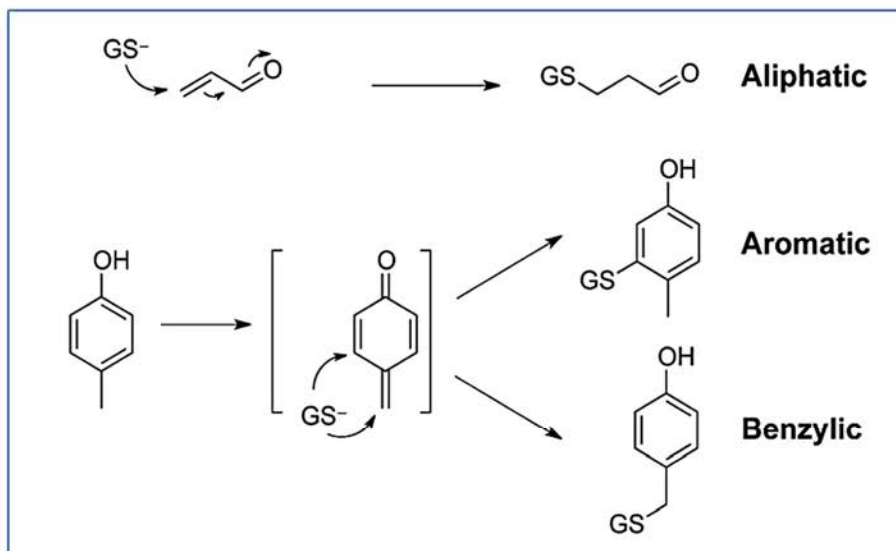
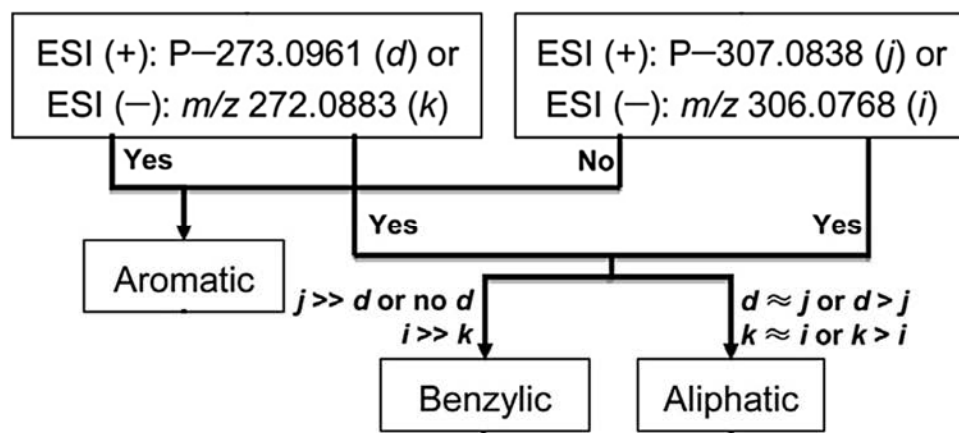
**Figure 6:** LC-QTOF-MS/MS spectra for the two GSH adduct peaks of interest observed for APAP; (A)  $m/z$  455.089 and (B)  $m/z$  471.119. The top, middle, and bottom panel for each spectrum represents collision energies of 10, 20, and 40 eV, respectively. The use of multiple collision energies allowed for optimum generation of identifying fragments.

**Table 2:** GSH adducts observed for all drugs tested, including proposed formula and composition and major ions.

Drug	Formula	Composition	Ions Observed <sup>a</sup>	Reference <sup>b</sup>
	C <sub>10</sub> H <sub>17</sub> N <sub>3</sub> O <sub>6</sub> S	GSH	<b>306.095</b> , 272.106( <i>k</i> ), 254.094, 210.103, 179.059, 160.020, 143.058( <i>b</i> ), 128.046( <i>f</i> )	
APAP1	C <sub>18</sub> H <sub>24</sub> N <sub>4</sub> O <sub>8</sub> S	D+GSH-2H	<b>455.089</b> , 272.089( <i>k</i> ), 254.078, 210.088, 182.028( <i>d</i> ), 143.045( <i>b</i> ), 128.046( <i>f</i> )	Dahlin et. al (1984)
APAP2	C <sub>18</sub> H <sub>24</sub> N <sub>4</sub> O <sub>9</sub> S	D+GSH+O-2H	<b>471.119</b> , 272.088( <i>k</i> ), 198.025 ( <i>d</i> ), 143.045( <i>b</i> ), 128.045( <i>f</i> )	Xie et. al (2013)
CLZ1	C <sub>28</sub> H <sub>34</sub> CIN <sub>7</sub> O <sub>6</sub> S	D+GSH-2H	<b>630.194</b> , 357.095( <i>d</i> ), 272.089( <i>k</i> ), 254.078, 143.046( <i>b</i> )	Zhu et. al. (2007)
CLZ2	C <sub>28</sub> H <sub>36</sub> CIN <sub>7</sub> O <sub>7</sub> S	D+GSH+O	<b>648.198</b> , 272.089( <i>k</i> ), 143.046( <i>b</i> )	Zhu et. al. (2007)
CLZ3	C <sub>23</sub> H <sub>24</sub> CIN <sub>5</sub> O <sub>7</sub> S	D+GSH+O-C <sub>5</sub> H <sub>10</sub> N <sub>2</sub>	<b>548.101</b> , 275.005( <i>d</i> ), 272.095( <i>k</i> ), 143.046( <i>b</i> )	na
COC1	C <sub>27</sub> H <sub>38</sub> N <sub>4</sub> O <sub>11</sub> S	D+GSH+O	<b>625.230</b> , 565.055, 384.821, 306.080( <i>j</i> ), 272.090( <i>k</i> ), 194.950, 143.046( <i>b</i> )	Schneider and DeCaprio (2013)
DZP1	C <sub>26</sub> H <sub>30</sub> CIN <sub>5</sub> O <sub>8</sub> S	D+GSH+O	<b>606.154</b> , 588.142, 315.039, 272.088( <i>k</i> ), 258.013, 210.089, 143.046( <i>b</i> )	na
MDMA1	C <sub>20</sub> H <sub>30</sub> N <sub>4</sub> O <sub>8</sub> S	D+GSH-CH <sub>2</sub>	<b>485.189</b> , 272.090( <i>k</i> ), 212.771( <i>d</i> ), 143.047( <i>b</i> ), 128.045( <i>f</i> )	Meyer et. al. (2014)
MDMA2	C <sub>21</sub> H <sub>30</sub> N <sub>4</sub> O <sub>8</sub> S	D+GSH-2H	<b>497.131</b> , 272.091( <i>k</i> ), 254.085, 143.047( <i>b</i> ), 128.046( <i>f</i> )	Meyer et. al. (2014)
MDMA3	C <sub>19</sub> H <sub>25</sub> N <sub>3</sub> O <sub>9</sub> S	D+GSH+O-C <sub>2</sub> H <sub>7</sub> N	<b>470.140</b> , 436.793, 272.090( <i>k</i> ), 197.030( <i>d</i> ), 143.046( <i>b</i> ), 128.045( <i>f</i> )	Meyer et. al. (2014)
MDPV1	C <sub>25</sub> H <sub>36</sub> N <sub>4</sub> O <sub>9</sub> S	D+GSH-CH <sub>2</sub>	<b>567.238</b> , 294.118( <i>d</i> ), 272.091( <i>k</i> )	Meyer et. al. (2014)
MDPV2	C <sub>21</sub> H <sub>29</sub> N <sub>3</sub> O <sub>9</sub> S	D+GSH-C <sub>5</sub> H <sub>8</sub> N	<b>498.172</b> , 272.089( <i>k</i> ), 225.060( <i>d</i> ), 143.046( <i>b</i> ), 139.995	na
MDPV3	C <sub>21</sub> H <sub>29</sub> N <sub>3</sub> O <sub>10</sub> S	D+GSH+O-C <sub>5</sub> H <sub>7</sub> N	<b>514.168</b> , 378.808, 272.103( <i>k</i> ), 241.068( <i>d</i> ), 143.056( <i>b</i> )	na
MOR1	C <sub>27</sub> H <sub>34</sub> N <sub>4</sub> O <sub>9</sub> S	D+GSH-OH	<b>589.219</b> , 316.102( <i>d</i> ), 306.077( <i>j</i> ), 272.089( <i>k</i> ), 210.089, 143.046( <i>b</i> ), 128.045( <i>f</i> )	Todaka et. al. (2005)
NAL1	C <sub>30</sub> H <sub>38</sub> N <sub>4</sub> O <sub>10</sub> S	D+GSH-2H	<b>645.249</b> , 306.094( <i>j</i> ), 272.105( <i>k</i> ), 210.089, 143.057( <i>b</i> ), 128.046( <i>f</i> )	na
NAL2	C <sub>30</sub> H <sub>40</sub> N <sub>4</sub> O <sub>11</sub> S	D+GSH+O	<b>663.260</b> , 390.157( <i>d</i> ), 358.184( <i>j</i> ), 306.093( <i>j</i> ), 272.105( <i>k</i> ), 210.089, 143.057( <i>b</i> ), 128.046( <i>f</i> )	na
OXY1	C <sub>28</sub> H <sub>36</sub> N <sub>4</sub> O <sub>10</sub> S	D+GSH-2H	<b>619.208</b> , 408.012, 306.077( <i>j</i> ), 272.958( <i>k</i> ), 210.089, 143.057( <i>b</i> ), 128.046( <i>f</i> )	na
OXY2	C <sub>28</sub> H <sub>34</sub> N <sub>4</sub> O <sub>11</sub> S	D+GSH+O-4H	<b>633.223</b> , 306.076( <i>j</i> ), 272.088( <i>k</i> ), 210.089, 143.057( <i>b</i> ), 128.046( <i>f</i> )	na
THC1	C <sub>31</sub> H <sub>45</sub> N <sub>3</sub> O <sub>9</sub> S	D+GSH+O-2H	<b>634.306</b> , 361.205( <i>d</i> ), 306.095( <i>j</i> ), 272.106( <i>k</i> ), 210.091, 143.058( <i>b</i> ), 128.046( <i>f</i> )	na
THC2	C <sub>31</sub> H <sub>45</sub> N <sub>3</sub> O <sub>10</sub> S	D+GSH+O <sub>2</sub> -2H	<b>650.301</b> , 377.199( <i>d</i> ), 343.193( <i>j</i> ), 306.094( <i>j</i> ), 272.106( <i>k</i> ), 210.091, 143.057( <i>b</i> ), 128.046( <i>f</i> )	na
THC3	C <sub>31</sub> H <sub>45</sub> N <sub>3</sub> O <sub>11</sub> S	D+GSH+O <sub>3</sub> -H	<b>666.297</b> , 393.195( <i>d</i> ), 359.190( <i>j</i> ), 306.094( <i>j</i> ), 272.106( <i>k</i> ), 210.091, 143.057( <i>b</i> ), 128.046( <i>f</i> )	na
THC4	C <sub>31</sub> H <sub>41</sub> N <sub>3</sub> O <sub>12</sub> S	D+GSH+O <sub>4</sub> -4H	<b>678.304</b> , 306.095( <i>j</i> ), 272.106( <i>k</i> ), 210.091, 143.058( <i>b</i> ), 128.046( <i>f</i> )	na

<sup>a</sup>Molecular ion in bold; letters in parentheses refer to characteristic GSH fragments according to nomenclature of Xie et al. (2013).

<sup>b</sup>Literature reference for previously reported adduct; na – not previously reported.



Fragment	Negative Mode m/z
b	143.0451
d	P-273.0961
f	128.0342
i	306.0765
j	P-307.0838
k	272.0883

Xie, C., Zhong, D. F., and Chen, X. Y. A fragmentation-based method for the differentiation of glutathione conjugates by high-resolution mass spectrometry with electrospray ionization. *Analytica Chimica Acta* 788, 89-98. 2013.

**Figure 7:** Details on approach used to interpret QTOF MS/MS data for identification of drug-GSH adduction products and location of thiol linkage to drug molecule.

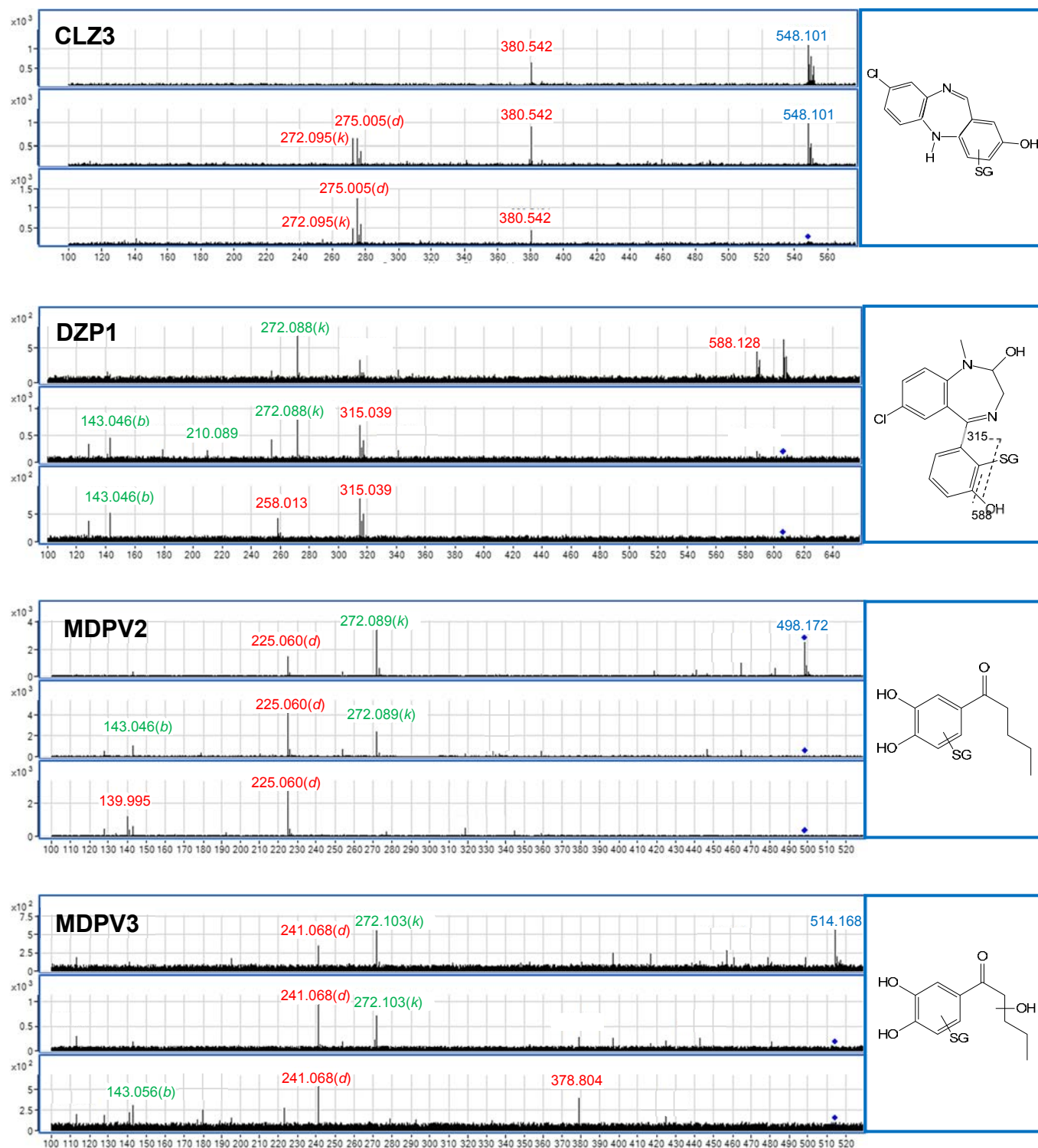


**Figure 8:** MS/MS spectra for all 12 previously unreported adducts. The molecular ion is represented in blue, GSH-specific peaks in green, and structurally significant peaks for GSH-containing compounds in red. Proposed structures for 9 of the 12 adducts are also shown with GSH linkage indicated.

This resource was prepared by the author(s) using Federal funds provided by the U.S. Department of Justice. Opinions or points of view expressed are those of the author(s) and do not necessarily reflect the official position or policies of the U.S. Department of Justice.

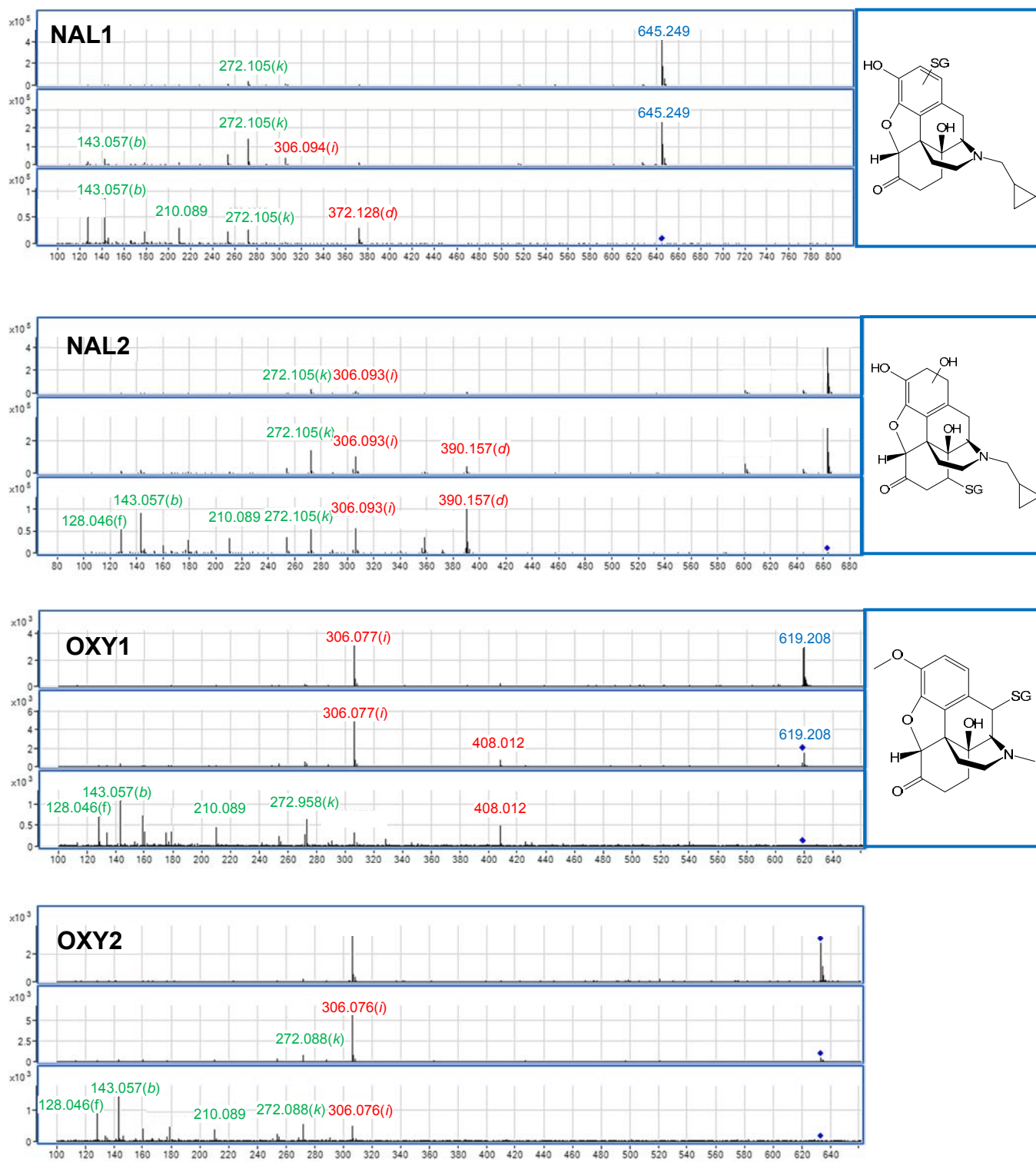


**Figure 8: continued**



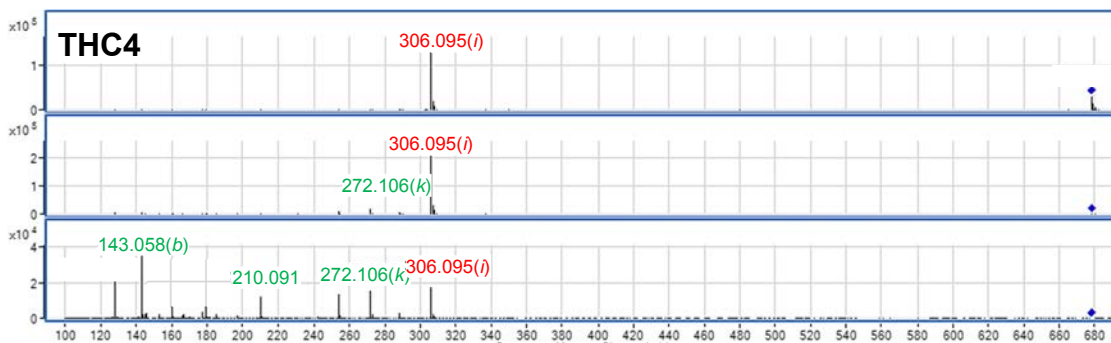
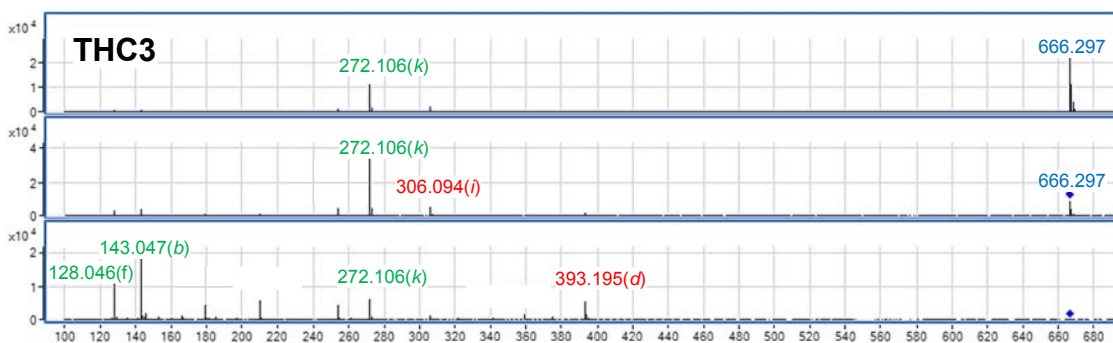
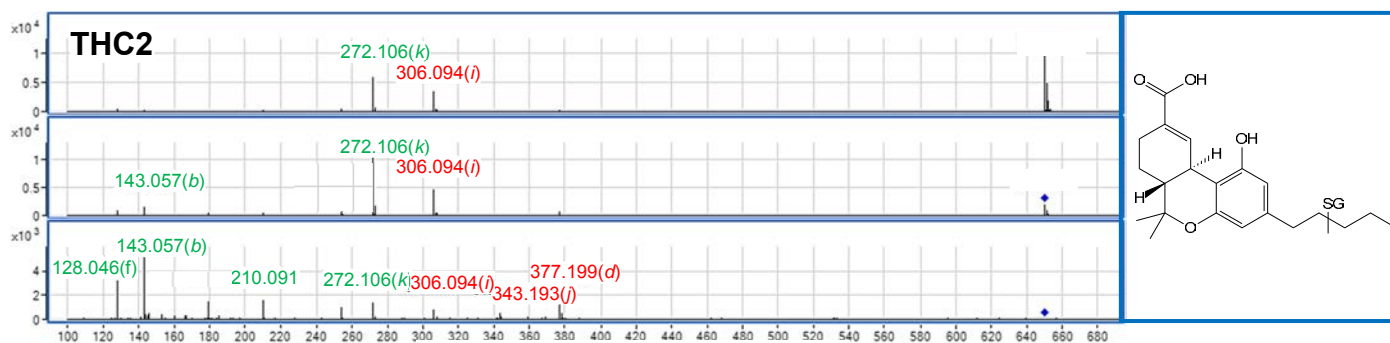
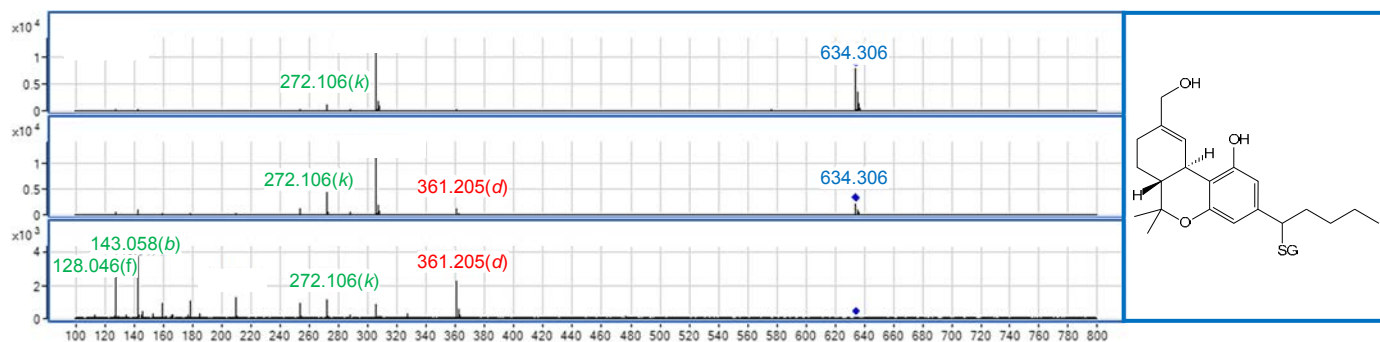


**Figure 8:** continued



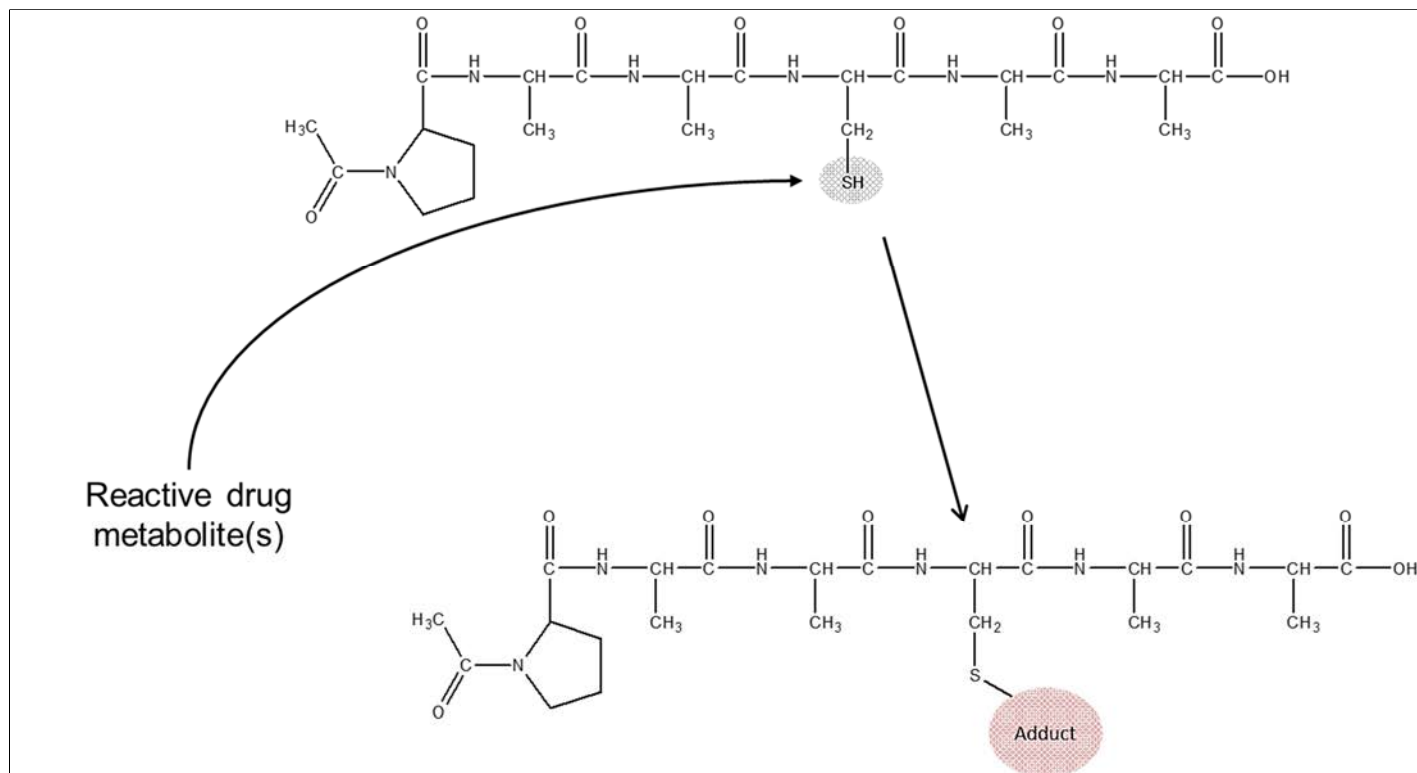
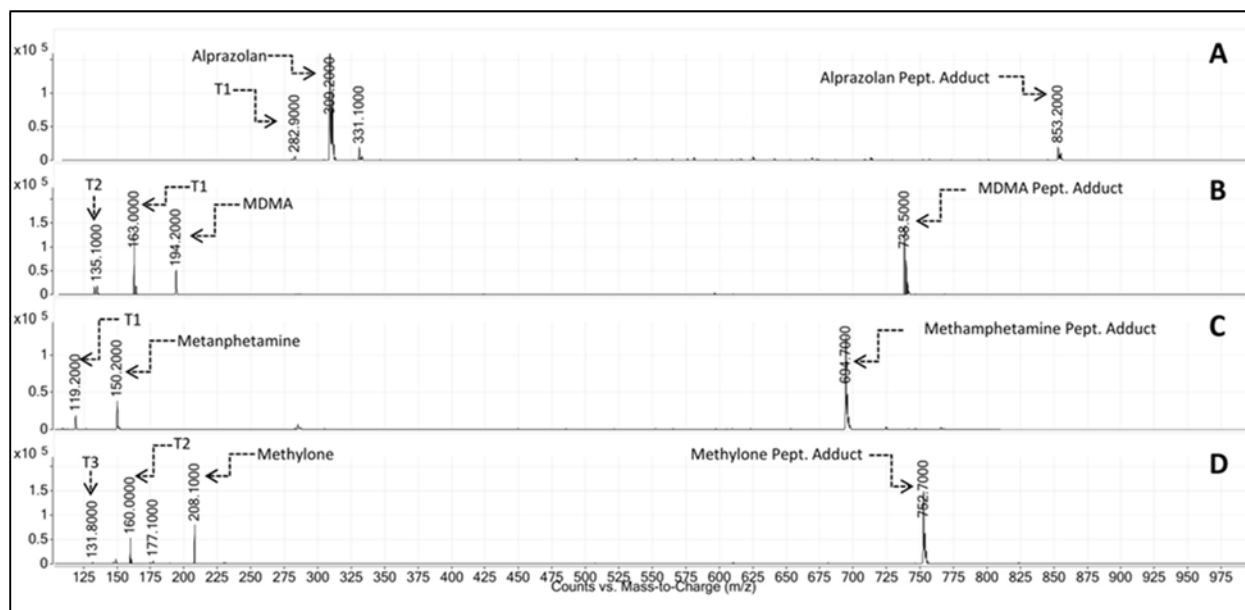
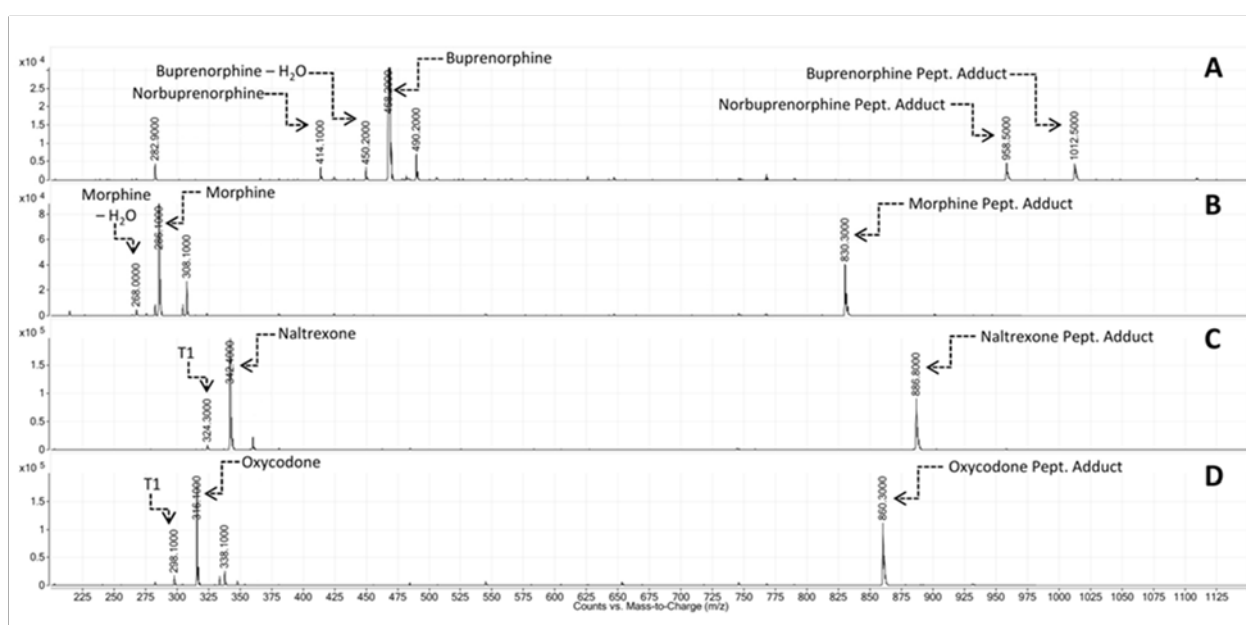
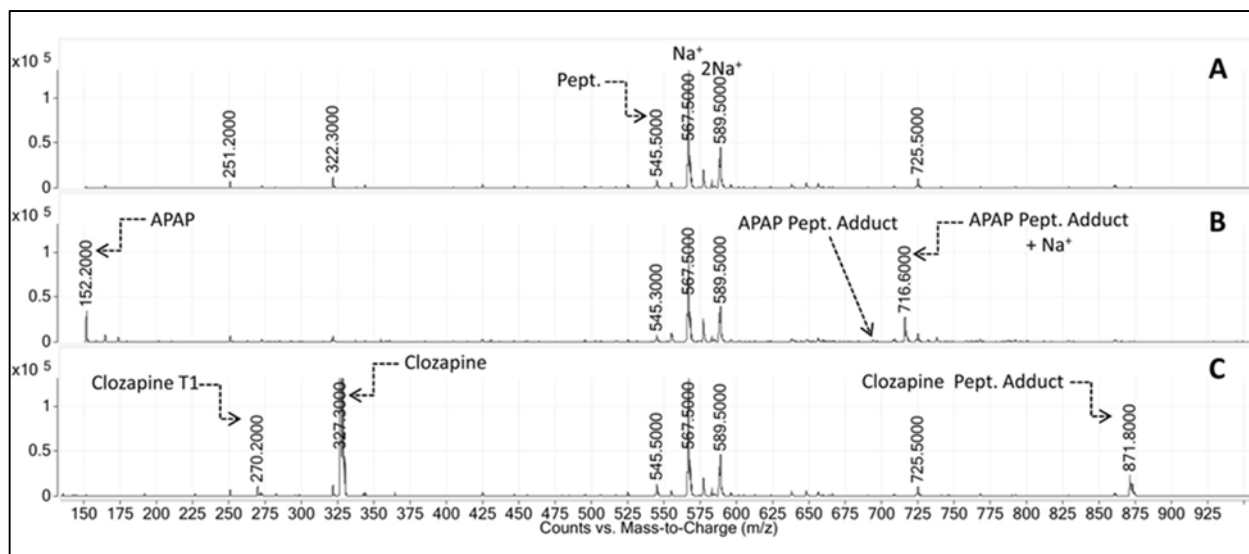


**Figure 9:** Scheme illustrating adduction of model Cys peptide by reactive drug metabolites.

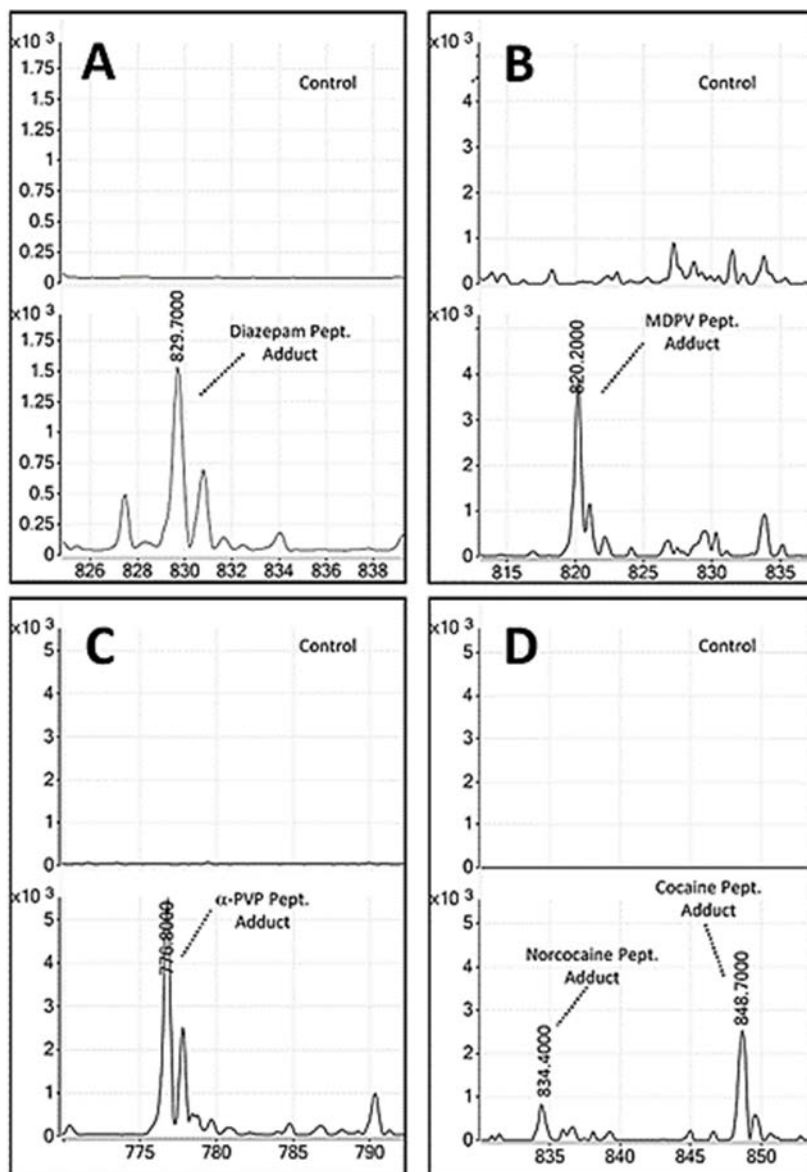
**Table 3:** Summary of MS results for model peptide modification by reactive drug metabolites

Drug	Parent Drug [M+H] <sup>+</sup>	Adducted Peptide [M+H] <sup>+</sup>	<sup>1</sup> Adducted Peptide MS/MS Spectra
APAP	152.2	694.5	Yes
CLZ	327.2	871.8	Yes
ALP	309.1	853.2	Yes
BUP	468.3	1012.5	Yes
COC	304.3	848.1	No
DZP	285.2	828.4	Yes
MDMA	194.2	738.7	Yes
MDPV	276.1	820.0	No
MET	150.2	694.7	Yes
META	310.1	849.7	No
METY	208.2	752.7	Yes
MOR	286.1	830.3	Yes
NAL	342.2	886.8	Yes
OXY	316.1	860.3	Yes
$\alpha$ -PVP	232.3	776.4	No
$\Delta^9$ -THC	315.2	859.6	No

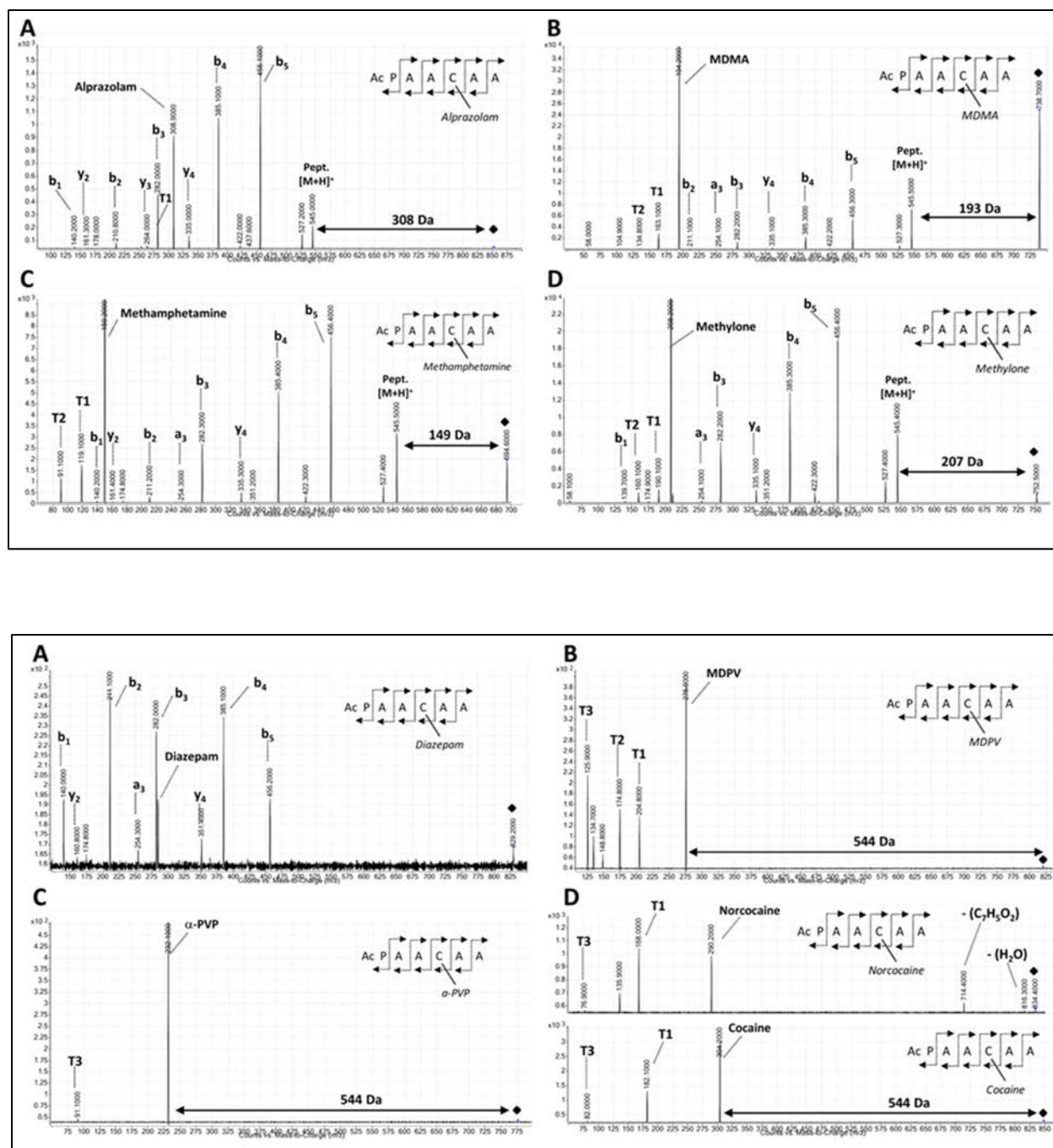
<sup>1</sup> Drugs for which adequate MS/MS spectra of the adducts were obtained are labeled as (Yes). Low intensity adduct peaks and/or adducts representing poorly resolved MS/MS spectra are labeled as (No).



**Figure 10: ESI-MS spectra of the synthetic model peptide Ac-PAACAA adduction by selected drugs, showing parent drugs and GED products, along with adducted peptide molecular ion.**



**Figure 11:** ESI-MS spectra of adducted by (A) diazepam, (B) MDPV, (C)  $\alpha$ -PVP, and (D) norcocaine and cocaine. The upper spectra show the control or unmodified peptide and the bottom spectra the appearance of new peaks of the adducted peptide.



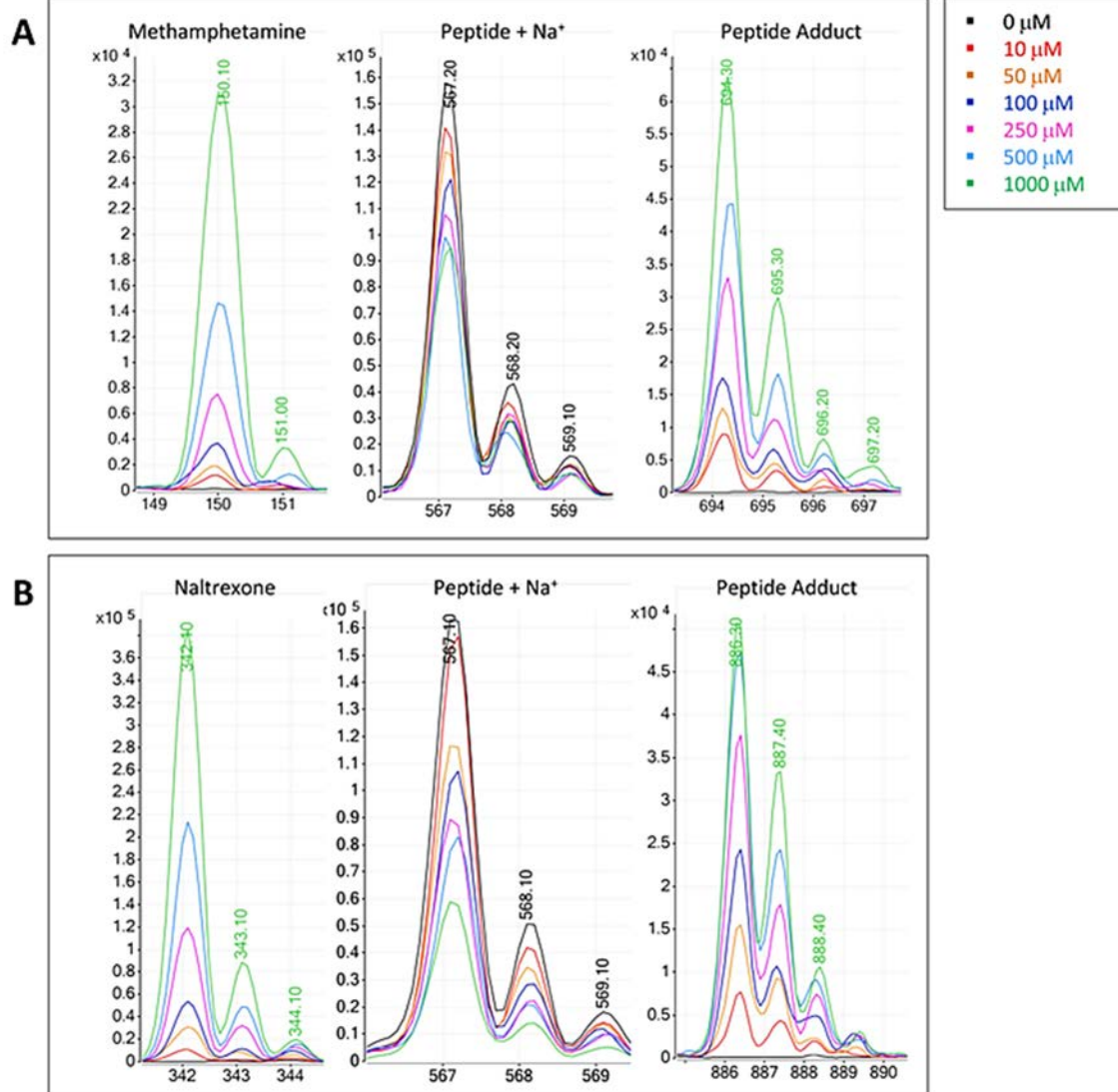


**Figure 13:** ESI-MS spectrum of model peptide adduction by different concentrations of methamphetamine and naltrexone. The peak abundance of the peptide adducts increases at higher drug concentrations while the peak abundance of the unmodified peptide decreases at higher drug concentrations.

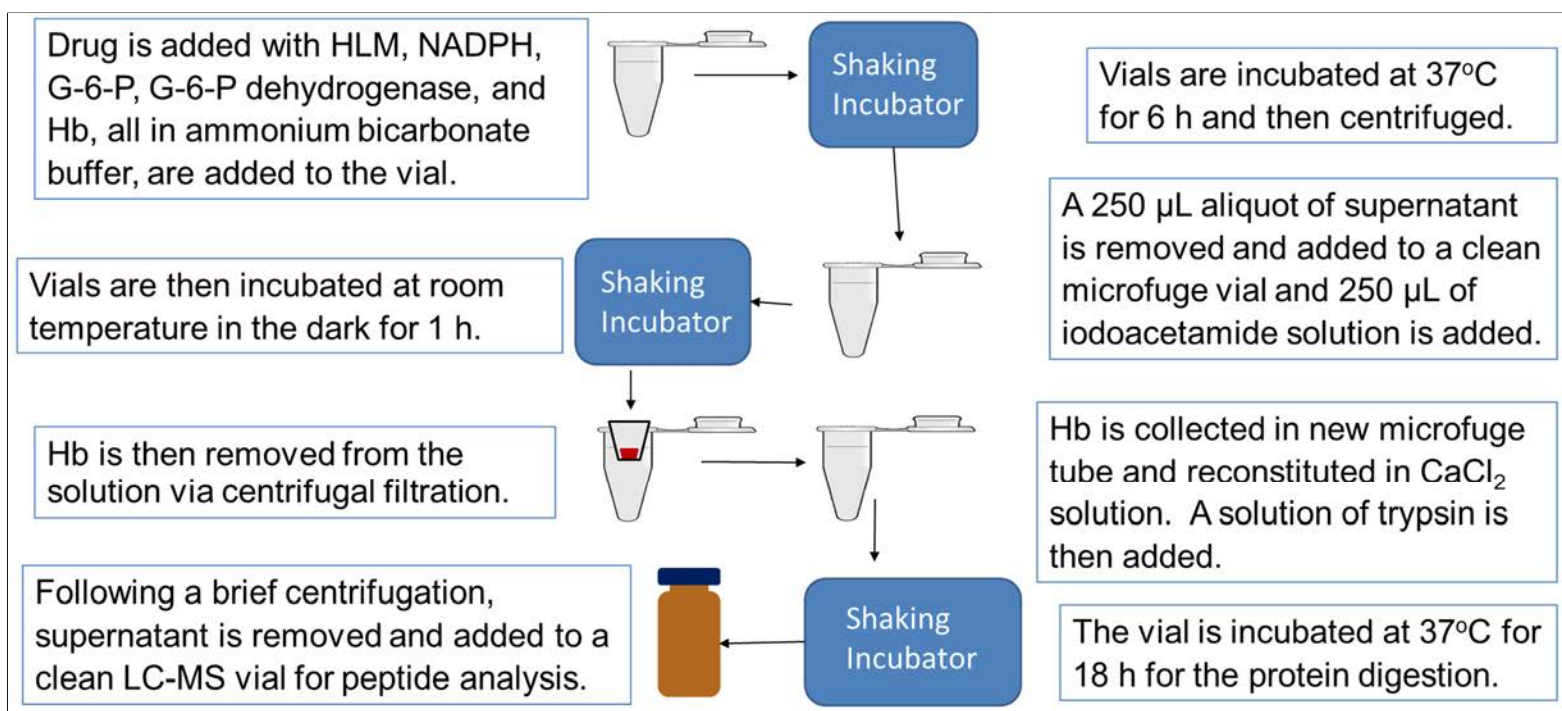


**Figure 14:** Details of the *in vitro* drug metabolism/trapping assay used for protein (human hemoglobin) adduction studies.

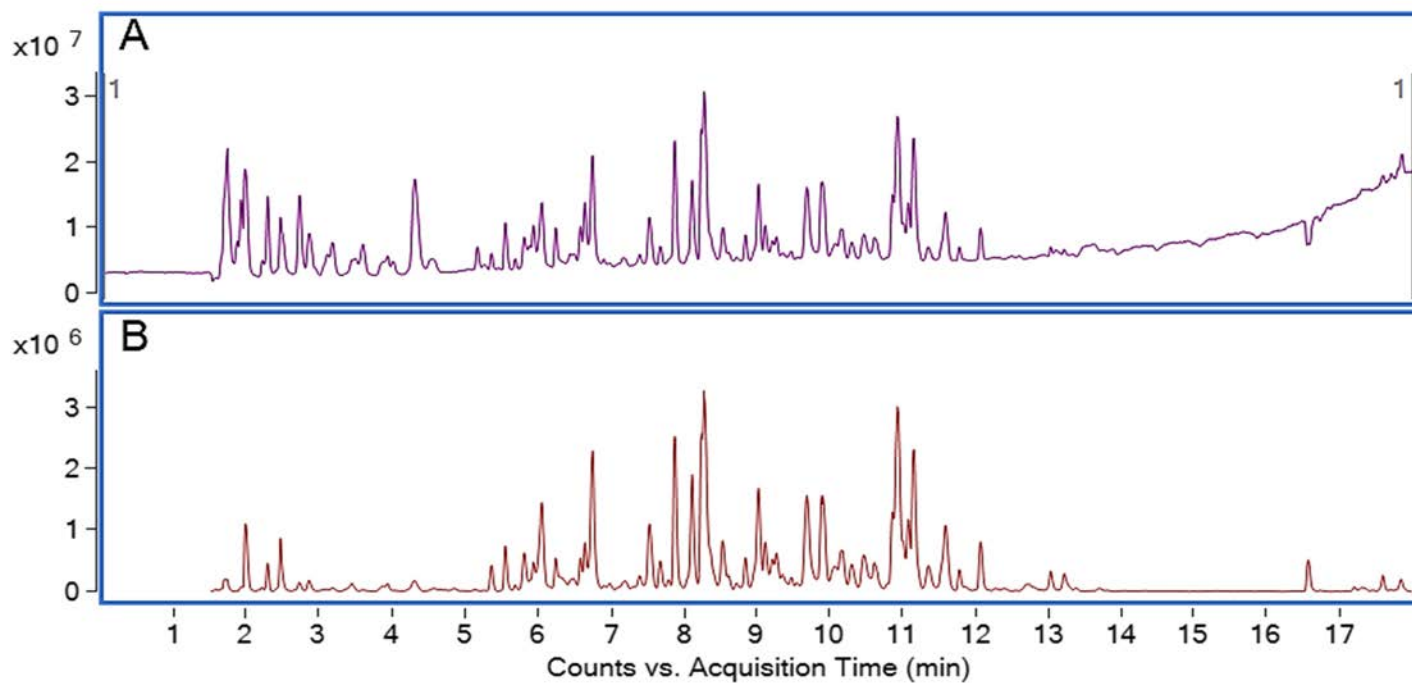


**Figure 15:** Total Ion Chromatogram (A) and Targeted Compound Chromatogram (B) for tryptic peptide digest of APAP-adducted human Hb assay mixture.



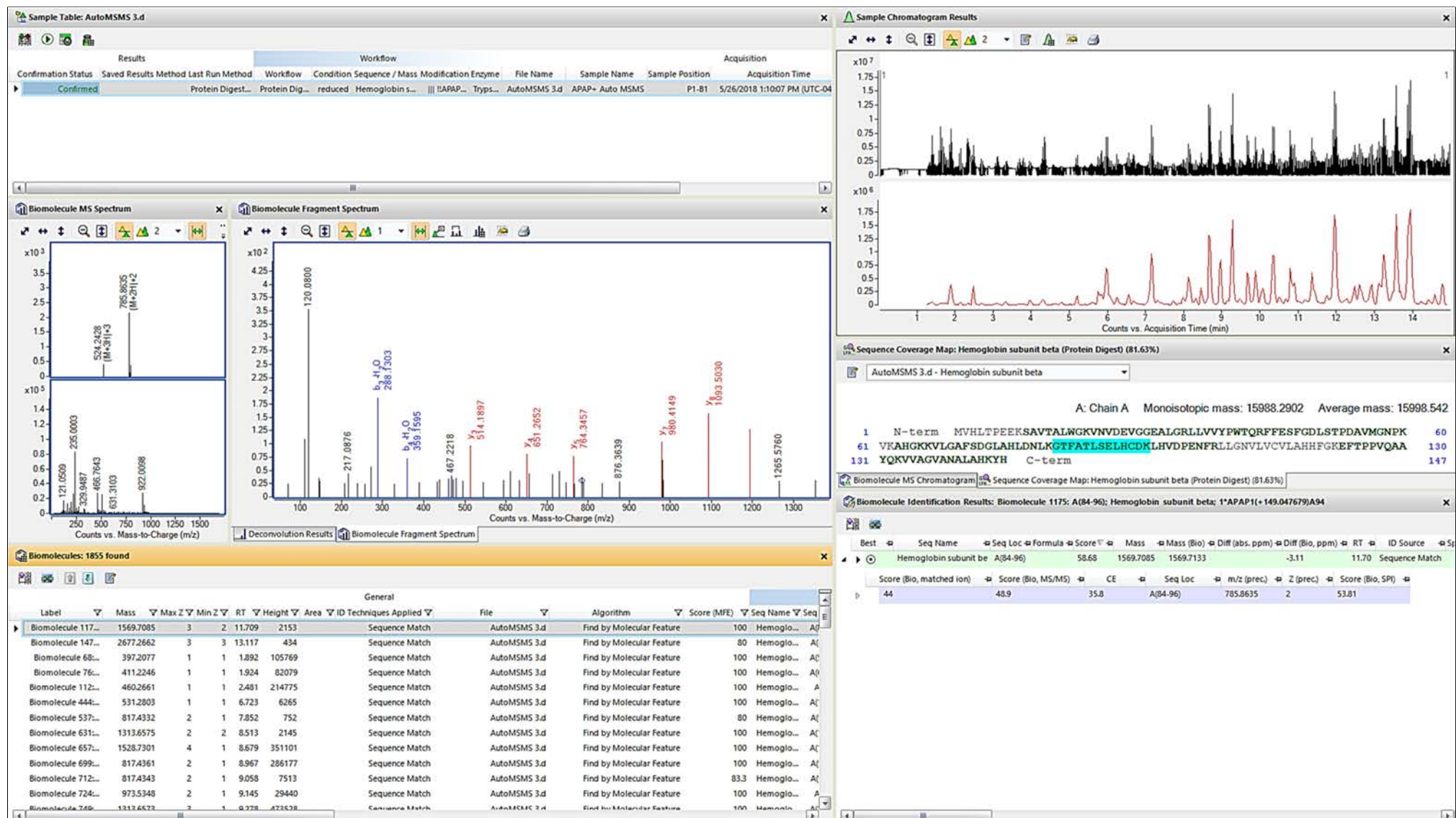
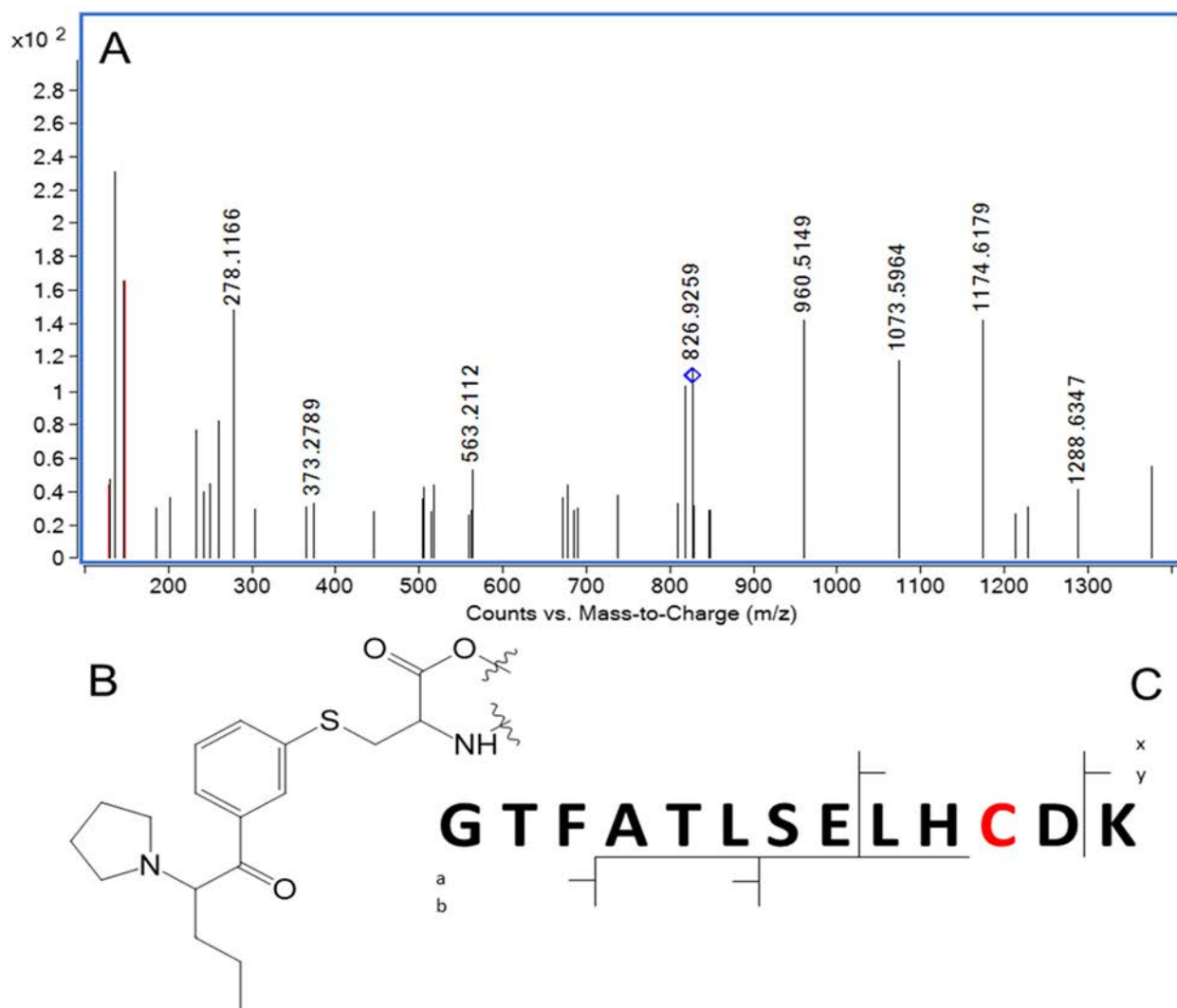


**Figure 16:** Illustration of peptide data analysis using Bioconfirm to identify APAP adduction at  $\beta^{93}\text{Cys}$  moiety of human Hb. Middle panel shows MS/MS spectrum of GTFATLSELHCDK tryptic peptide showing characteristic y- and b-fragment ions expected with APAP adduction at  $\beta^{93}\text{Cys}$ .

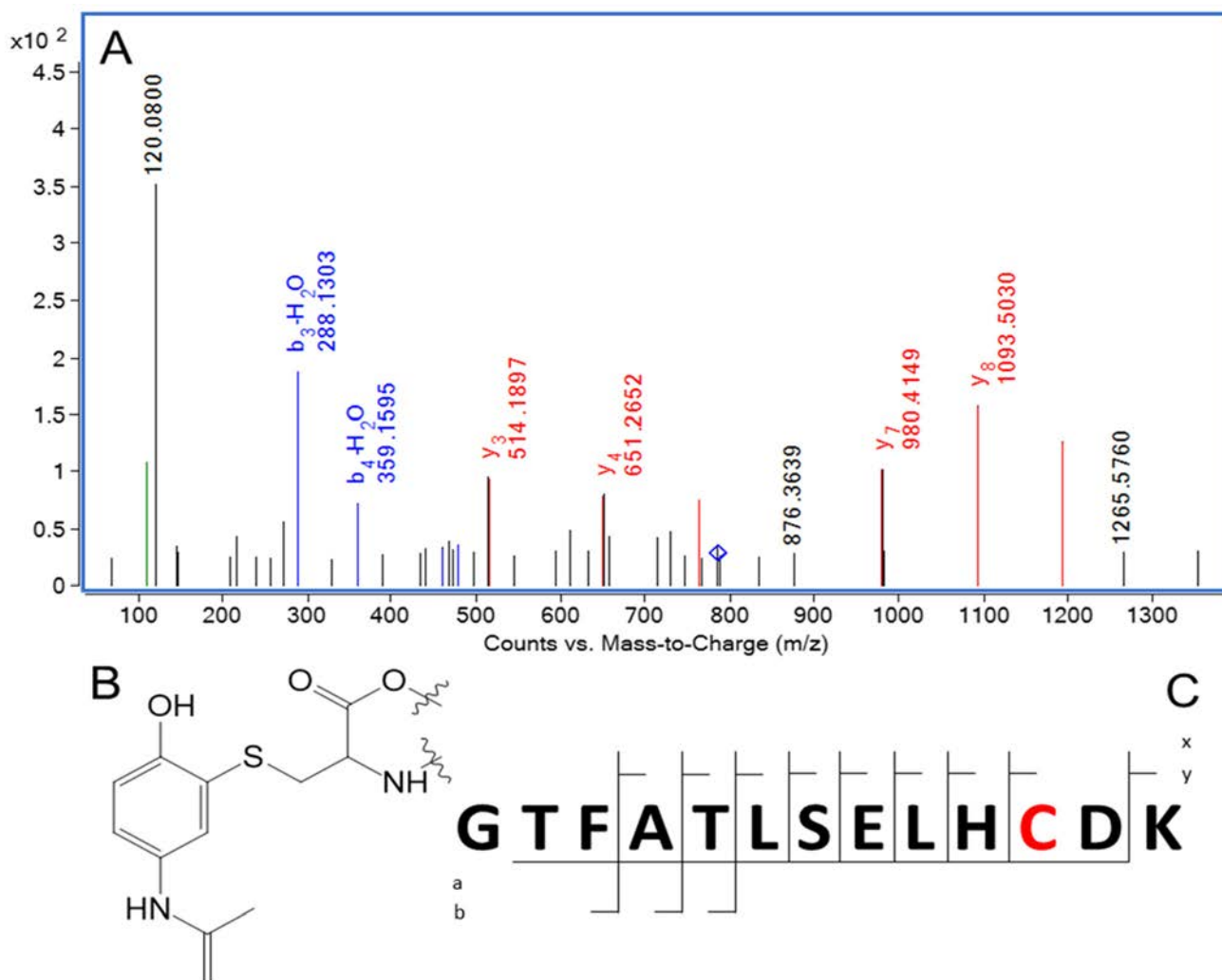
**Table 4:** Summary of QTOF-MS (gray) and -MS/MS (green) data for Hb adducts confirmed for six of the drugs examined in the project. Data indicates specific Cys thiol modified, other modifications detected, and mass difference from predicted.

	Adduct	Adduction Site	Other Mods	$\Delta m/z$ (ppm)	Adducted Peptide Mass
1	APAP1	Hb $\beta^{93}$	none	2.93	1569.718
2	APAP1	Hb $\beta^{112}$	none	-3.29	1868.0069
3	$\alpha$ -PVP1	Hb $\beta^{93}$	none	-3.63	1651.822
4	METH1	Hb $\beta^{93}$	none	-4.63	1597.7632
5	METH1	Hb $\alpha^{104}$	1Hydrox.+1Acetyl.	3.36	3171.7261
6	METH1	Hb $\beta^{93}$	1Acetyl.	5.14	1609.7728
7	NAL1	Hb $\beta^{93}$	none	-0.61	1759.8117
8	OXY1	Hb $\beta^{93}$	none	3.57	1733.8033
9	OXY1	Hb $\alpha^{104}$	1Hydrox.+1Acetyl.	7.84	3337.7682
10	THC1	Hb $\beta^{93}$	1Hydrox.+1Acetyl.	4.34	2914.4338*
11	THC2	Hb $\beta^{93}$	1Hydrox.	-7.16	1780.8466



Fragment Mass	Fragment
129.1022	K
130.0863	y <sub>1</sub> -NH <sub>3</sub>
147.1128	y <sub>1</sub>
278.1499	a <sub>3</sub>
373.2082	ATLS
562.2984	LSELH-H <sub>2</sub> O
563.3188*	a <sub>6</sub>
818.4068 <sup>+2</sup>	MH-NH <sub>3</sub> <sup>+2</sup>
826.9201 <sup>+2</sup>	MH <sup>+2</sup>
846.4519	y <sub>5</sub>

**Figure 17:** QTOF MS/MS spectrum, adduct localization, and structure (top panel) and confirmed characteristic fragments (bottom panel) for  $\alpha$ -PVP adduct with human Hb.



Fragment Mass	Fragment	Fragment Mass	Fragment
110.0713	H	593.3293*	TFATLS-28
120.0808	F	633.2573	y <sub>4</sub> -H <sub>2</sub> O
145.0972	AT-28	651.2678	y <sub>4</sub>
147.1128	y <sub>1</sub>	729.2784	ELHC(+149.06)D-H <sub>2</sub> O
217.0819	SE	747.3254	y <sub>5</sub> -NH <sub>3</sub>
257.6081 <sup>+2*</sup>	y <sub>3</sub> <sup>+2</sup>	764.3519	y <sub>5</sub>
288.1343	b <sub>3</sub> -H <sub>2</sub> O	785.8701 <sup>+2</sup>	MH <sup>+2</sup>
359.1714	b <sub>4</sub> -H <sub>2</sub> O	835.456	TFATLSEL-28
433.2445	FATL	876.368	y <sub>6</sub> -NH <sub>3</sub>
439.23	SELH-28	980.4265	y <sub>7</sub>
460.2191	b <sub>5</sub> -H <sub>2</sub> O	982.4993	TFATLSELH-H <sub>2</sub> O
467.2249	SELH	1093.5106	y <sub>8</sub>
478.2296	b <sub>5</sub>	1194.5583	y <sub>9</sub>
496.1984	y <sub>3</sub> -H <sub>2</sub> O	1265.5954	y <sub>10</sub>
514.2089	y <sub>3</sub>		

**Figure 18:** QTOF MS/MS spectrum, adduct localization, and structure (top panel) and confirmed characteristic fragments (bottom panel) for APAP adduct with human Hb.

## **Conference Presentations**

Gilliland, R.A. and DeCaprio, A.P. (2018). Analysis and characterization of in vitro glutathione adducts formed with drugs of abuse". *Pittsburgh Conference on Analytical Chemistry and Applied Spectroscopy (Pittcon)*, Orlando, FL; February 26 - March 1.

Gilliland, R.A. and DeCaprio, A.P. (2018). Mass spectrometric approach to the analysis of covalent modifications of blood proteins by drugs of abuse. *American Academy of Forensic Sciences 70<sup>th</sup> Annual Meeting*, Seattle, WA; February 19-23.

Gilliland, R.A., Moller, C., and DeCaprio, A.P. (2017). LC-MS/MS based analysis of in vitro covalent modifications of glutathione and peptide thiols by drugs of abuse. *American Academy of Forensic Sciences 69<sup>th</sup> Annual Meeting*, New Orleans, LA; February 13-18.

Gilliland, R.A., Moller, C., and DeCaprio, A.P. (2017). LC-MS/MS based analysis of in vitro covalent modifications of glutathione and peptide thiols by drugs of abuse. *FIU Graduate Student Appreciation Week Scholarly Forum*, Miami, FL.

Gilliland, R.A., Moller, C., and DeCaprio, A.P. (2017). LC-MS/MS based analysis of in vitro covalent modifications of glutathione and peptide thiols by drugs of abuse. *6<sup>th</sup> Annual IFRI Forensic Science Symposium*, Miami, FL; May 9-10.

Gilliland, R.A. and DeCaprio, A.P. (2018). Analysis of drug-protein modifications in forensic toxicology. *Invited talk presented at the Pittsburgh Conference on Analytical Chemistry and Applied Spectroscopy (Pittcon)*, Orlando, FL; February 26 - March 1.

DeCaprio, A.P., Gilliland, R.A., and Moller, C. (2017). Novel blood protein modification assay for retrospective detection of drug exposure. *Invited talk presented at the American Academy of Forensic Sciences 69<sup>th</sup> Annual Meeting*, New Orleans, LA; February 14.

## **Publications**

Gilliland, R.A., Möller, C., and DeCaprio, A.P. (2018). LC-MS/MS based detection and characterization of covalent glutathione modifications formed by reactive drug of abuse metabolites. *Xenobiotica*, *in press*.

Möller, C., Gilliland, R.A., Arroyo-Mora, L., and DeCaprio, A.P. (2018). In vitro peptide-based assay for the detection of thiol adducts of drugs of abuse. *Bioanalysis*, *in preparation*.

Gilliland, R.A. and DeCaprio, A.P. (2018). Formation of covalent thiol adducts in human hemoglobin by reactive drug metabolites. *Chemical Research in Toxicology*, *in preparation*



RESEARCH ARTICLE



## LC-MS/MS based detection and characterization of covalent glutathione modifications formed by reactive drug of abuse metabolites

R. Allen Gilliland, Carolina Möller and Anthony P. DeCaprio

Department of Chemistry & Biochemistry and International Forensic Research Institute, Florida International University, Miami, FL, USA

### ABSTRACT

1. Conjugation with the tripeptide glutathione (GSH) is a common mechanism of detoxification of many endogenous and exogenous compounds. This phenomenon typically occurs through the formation of a covalent bond between the nucleophilic free thiol moiety of GSH and an electrophilic site on the compound of interest.
2. While GSH adducts have been identified for many licit drugs, there is a lack of information on the ability of drugs of abuse to adduct GSH. The present study utilized a metabolic assay with GSH as a nucleophilic trapping agent to bind reactive drug metabolites formed *in situ*.
3. Extracted ion MS spectra were collected via LC-QqQ-MS/MS for all potentially significant ions and examined for fragmentation common to GSH-containing compounds, followed by confirmation of adduction and structural characterization performed by LC-QTOF-MS/MS.
4. In addition to the two positive controls, of the 14 drugs of abuse tested, 10 exhibited GSH adduction, with several forming multiple adducts, resulting in a total of 22 individual identified adducts. A number of these are previously unreported in the literature, including those for diazepam, naltrexone, oxycodone and  $\Delta^9$ -THC.

### ARTICLE HISTORY

Received 8 May 2018  
Revised 20 July 2018  
Accepted 21 July 2018

### KEYWORDS

Glutathione; LC-MS/MS;  
drugs of abuse; adducts

### Introduction

Phase I and Phase II metabolic processes generally form more polar metabolites of xenobiotics and are typically a means of detoxification and preparation for excretion. Phase I metabolism, such as hydroxylation or epoxidation, refers to a number of reactions a xenobiotic may undergo where a relatively small modification occurs which may slightly increase hydrophilicity. Phase II metabolism, such as glucuronidation, refers to reactions where hydrophilicity is substantially increased by the addition of a large polar moiety. These metabolic products do not typically cause harm to the endogenous cellular components in their vicinity. However, in some cases reactive intermediates may also be formed, which may then modify nearby macromolecules to form covalent adducts, primarily through electrophilic–nucleophilic interactions (Attia, 2010; Miller & Miller, 1965). The formation of these modifications can create a potential for organ-specific toxicity (Ikehata et al., 2008; Lu et al., 2009) or, alternatively, can be innocuous. In either case, such adducts may also serve as biomarkers of exposure (Xie et al., 2013).

Metabolic trapping assays have been widely employed to study these possibly harmful products *in vitro*, particularly in pharmaceutical development where there is a need to

identify the potential for reactive metabolite production in candidate drugs (Thompson et al., 2011; Yamaoka & Kitamura, 2015). Such assays are designed to mimic Phase I and II metabolic processes in human cells (Evans et al., 2004). When a metabolic assay is used for the purpose of examining reactive metabolite formation, a trapping agent must be added as a target for covalent modification (Meneses-Lorente et al., 2006). Trapping agents are typically any one of numerous, primarily nucleophilic and generally small, molecules that can bind covalently to reactive intermediates, preventing further metabolism and preserving the structure of the otherwise unstable compound (Schneider & DeCaprio, 2013). Examples of trapping agents used in these assays include glutathione (GSH) (Schadt et al., 2015; Yamaoka & Kitamura, 2015), N-acetylcysteine (Schneider & DeCaprio, 2013), and cyanide (Evans et al., 2004).

Glutathione (GSH) is a tripeptide which consists of glutamic acid, cysteine and glycine that is found endogenously in human cells at concentrations ranging up to 10 mM (Shimizu et al., 2002). GSH contains a free thiol moiety that acts as a reactive nucleophilic site and that has been shown to covalently bind to electrophiles *in vivo* (Dahlin et al., 1984; Zhu et al., 2007). The capability of GSH to bind to reactive

metabolites allows it to function as one of the primary cellular defenses against electrophilic/oxidative stress and damage. Because of GSH's reactivity and prevalence in the body, GSH adducts have also been used as markers to identify, analyze, and monitor exposure to and excretion of compounds of interest (Blair, 2010; DeCaprio, 1997; Meyer et al., 2014; Todaka et al., 2005). The chemistry and structure of GSH make it an ideal candidate for a trapping agent when utilized in an *in vitro* metabolic assay (Gomez-Lechon et al., 2016; Inoue et al., 2009; Kalgutkar, 2011).

Drug abuse is a prominent and on-going problem in the United States and globally. Abused drugs can be either licit or illicit compounds which, when ingested, provide a desired sensation to the user. The effect may be caused by either the parent drug or a metabolite which is transported throughout the body, ultimately reaching the brain as the primary pharmacological target. Many stable metabolites of commonly abused drugs are known and have been characterized. However, there is a lack of research related to the formation of potentially reactive metabolic intermediates for most drugs of abuse and in particular, the ability of such metabolites to covalently modify endogenous nucleophilic sites, including those of cellular proteins. Nevertheless, evidence is available for certain abused drugs that reactive metabolites may be the cause of severe and unexpected reactions in the body (Capela et al., 2007; Kovacic & Cooksy, 2005). For example, it has been hypothesized that hepatic necrosis caused by cocaine may be the result of protein binding by reactive metabolites (Ndikum-Moffor et al., 1998). It has also been shown that thioester MDMA metabolites increase levels of quinone-protein products in neurons (Capela et al., 2007).

We have previously reported that cocaine can covalently modify free thiols in GSH and model peptides in an *in vitro* metabolic system (Schneider & DeCaprio, 2013). The aim of the present research was to expand upon this work to examine the potential of a representative set of 16 licit and illicit drugs to form reactive metabolites capable of covalent binding to GSH. This was accomplished by utilizing an *in vitro* trapping assay system and analyzing reaction products using liquid chromatography (LC) coupled with triple quadrupole (QQQ) and quadrupole time of flight (QTOF) mass spectrometry. Results demonstrated the formation of 22 individual covalent GSH adduct structures by reactive metabolites of 10 of the 16 drugs examined. In addition to confirming previously reported GSH modifications for several drugs, a number of novel adducts were identified for drugs not previously studied.

## Materials and methods

### Drugs selected for study

Table 1 lists the drugs selected for the study along with chemical formulas and exact masses. Figure 1 shows structures for all 16 drugs. The drugs of interest in this study were selected based on a known potential for addiction/dependence and prevalent usage, while also ensuring that various structural and pharmacological classes of drugs were

Table 1. Data for parent drugs tested for GSH adduction potential.

Drug	Formula	Exact mass (Da)
Acetaminophen (APAP)	C <sub>9</sub> H <sub>9</sub> NO <sub>2</sub>	151.063
Alprazolam (ALP)	C <sub>17</sub> H <sub>13</sub> ClN <sub>4</sub>	308.083
Buprenorphine (BUP)	C <sub>29</sub> H <sub>41</sub> NO <sub>4</sub>	467.304
Clonazepam (CLZ)	C <sub>18</sub> H <sub>13</sub> ClN <sub>2</sub>	326.130
Cocaine (COC)	C <sub>17</sub> H <sub>21</sub> NO <sub>4</sub>	303.147
Diazepam (DZP)	C <sub>16</sub> H <sub>13</sub> ClN <sub>2</sub> O	284.072
Methadone (META)	C <sub>21</sub> H <sub>27</sub> NO	309.209
Methamphetamine (METH)	C <sub>10</sub> H <sub>15</sub> N	149.120
Methylenedioxymethamphetamine (MDMA)	C <sub>11</sub> H <sub>15</sub> NO <sub>2</sub>	193.110
Methylenedioxypyrovalerone (MDPV)	C <sub>16</sub> H <sub>21</sub> NO <sub>3</sub>	275.152
Methylone (METY)	C <sub>11</sub> H <sub>15</sub> NO <sub>3</sub>	207.090
Morphine (MOR)	C <sub>17</sub> H <sub>19</sub> NO	285.137
Naltrexone (NAL)	C <sub>20</sub> H <sub>25</sub> NO <sub>4</sub>	341.163
Oxycodone (OXY)	C <sub>18</sub> H <sub>21</sub> NO <sub>4</sub>	315.147
$\alpha$ -Pyrrolidinopentiophenone ( $\alpha$ -PVP)	C <sub>12</sub> H <sub>17</sub> NO	231.162
$\Delta^9$ -Tetrahydrocannabinol (THC)	C <sub>21</sub> H <sub>30</sub> O <sub>2</sub>	314.225

represented in the final list. All of the selected drugs are examples of compounds which may be identified in authentic specimens from law enforcement cases, rehabilitation centers, correctional facilities and outpatient therapy. In addition, two licit drugs, acetaminophen and clonazepam, were chosen as positive controls, since they have both been previously shown to form metabolites that readily adduct with GSH and other nucleophiles (Dahlin et al., 1984; Guengerich, 2003; Zhu et al., 2007).

### Materials

Drug abbreviations are as shown in Table 1. APAP, NAL and OXY were purchased from Sigma-Aldrich (St. Louis, MO); CLZ was purchased from Alfa Aesar (Haverhill, MA); COC was purchased from Cerilliant (Round Rock, TX); DZP and MOR were purchased from Research Biochemical International (Natick, MA); MDMA and THC were both purchased from Lipomed (Cambridge, MA); MDPV was purchased from Cayman Chemical (Ann Arbor, MI). COC and THC were obtained as standard solutions in methanol and ethanol, respectively. The remaining drugs were obtained as neat powders, and standard solutions with a concentration of 1 mg/mL in methanol (MeOH) were created and stored at -20 °C, the exceptions being NAL and APAP. For NAL, a 1 mg/mL solution was created in Optima™ grade water and the solution was stored at 4 °C and remade every four weeks. A fresh 1 mg/mL solution of APAP in MeOH was created daily as needed. Nicotinamide adenine dinucleotide phosphate tetrasodium salt (NADPH) was purchased from Merck Millipore (Billerica, MA); glucose-6-phosphate sodium salt (G6P), anhydrous MgCl<sub>2</sub>, and glucose-6-phosphate dehydrogenase from baker's yeast (G6PD) were all purchased from Sigma-Aldrich; reduced glutathione (GSH) was purchased from ThermoFisher Scientific (Hampton, NH). Pooled, mixed-gender human liver microsomes (HLM) with concentration of 20 mg protein/mL were purchased from XenoTech (Kansas City, KS). GPD and HLM were received as solutions with concentrations of 200 units/mg and 20 mg protein/mL, respectively. All other solvents and chemicals were from ThermoFisher Scientific.



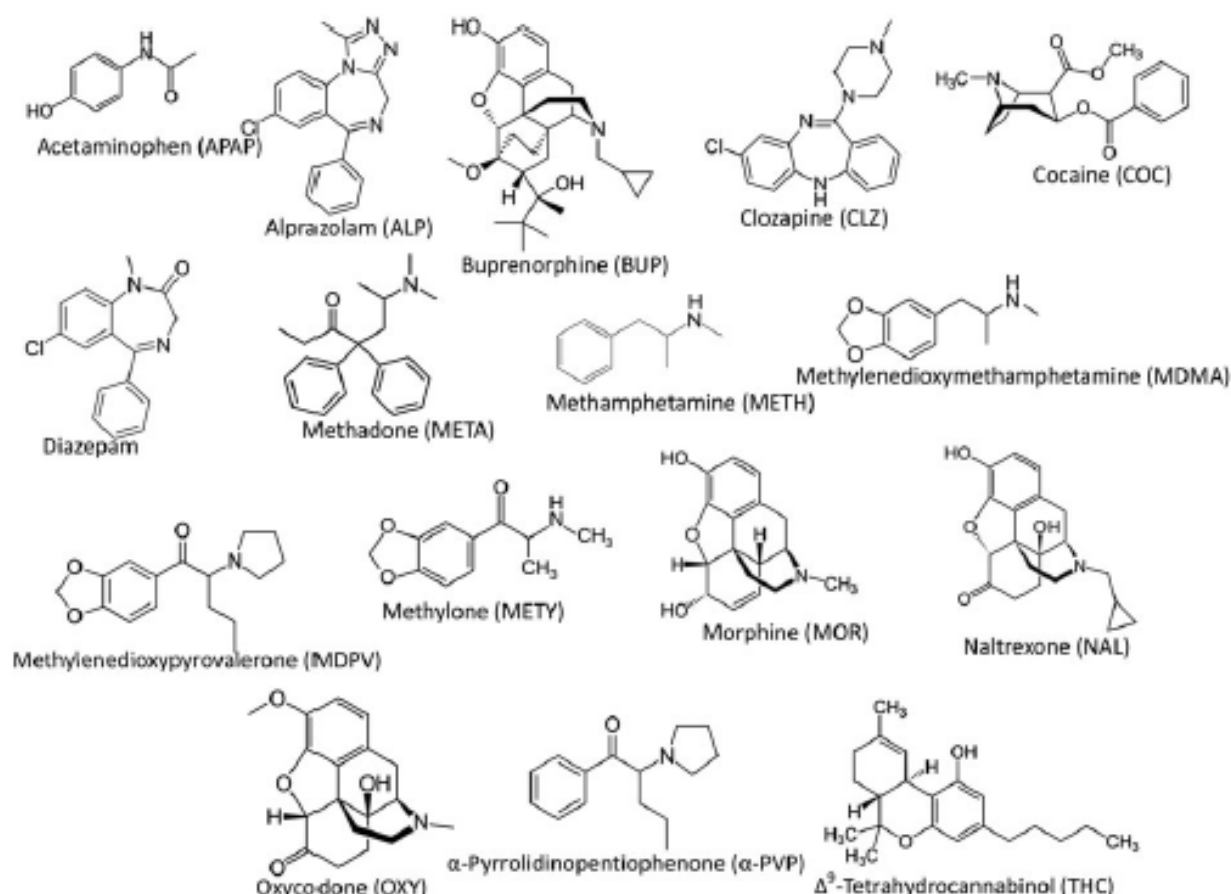


Figure 1. Structures for all 16 of the drugs of interest in this study. Each drug is labeled with its abbreviation as outlined in Table 1.

### Generation and trapping of reactive metabolites

Trapping assays were modified from previously published methods (Meyer et al., 2014; Schneider & DeCaprio, 2013). Briefly, components of the *in vitro* trapping assay were combined in a total assay volume of 125  $\mu$ L of 50 mM sodium phosphate buffer, pH 7.4, at the following final concentrations: 1000  $\mu$ M drug of interest, 1 mg/mL HLM, 3 mM  $MgCl_2$ , 2 mM NADPH, 3 mM G6P, 0.4 U/mL G6PD and 2 mM GSH. Assay components without GSH were first combined in a microfuge vial and vortexed briefly to ensure uniformity, followed by a pre-incubation of 15 min at 37  $^{\circ}$ C. GSH was then added to complete the assay and achieve final assay volume, and vials were once again vortexed to ensure proper mixing. Incubation then ensued at 37  $^{\circ}$ C for 3 h. Upon completion of incubation, vials were immediately centrifuged at 15,000 g at 4  $^{\circ}$ C for 30 min. Following centrifugation, 100  $\mu$ L aliquots of supernatant were removed from each vial and placed in separate, clean LC vials.

### MS analysis

#### General LC-MS parameters

Analysis by LC-QqQ-MS was performed on an Agilent 1290 Infinity UHPLC coupled to an Agilent 6460 QqQ MS. Analysis by LC-QTOF-MS was performed on an Agilent 1290 Infinity UHPLC coupled to an Agilent 6530 QTOF MS. Both instruments utilized Agilent Jet Streaming electrospray ionization

(ESI) set to negative mode polarity. The column utilized was an Agilent Zorbax Eclipse Plus  $C_{18}$  rapid resolution HD. A biphasic elution system consisting of eluent A: Optima<sup>TM</sup> grade water with 0.1% acetic acid, and B: 95% acetonitrile, 4.9% Optima<sup>TM</sup> grade water, and 0.1% acetic acid was utilized. The pump timetable was as follows: 5% B hold for 1 min, 5% to 100% B ramp from 1 to 14 min, 100% B hold for 2 min, followed by a 3-min post-time for reequilibration to initial conditions for next injection.

#### Initial detection of adduction products via QqQ-MS

Analysis by QqQ-MS of metabolic assay reaction products was performed using a precursor ion scan set to identify the precursor ions for any fragments with  $m/z$  272, a common and indicative product of GSH, corresponding to GSH less the sulfur atom (Dieckhaus et al., 2005). The scan took place over the mass range  $m/z$  400–800 to avoid interference from unreacted GSH and to maximize detection of likely adducts for all drugs. Fragmentor voltage was set to 120 V and collision energy was set to 10 eV. Peaks were determined to be potentially significant if they had an unscaled abundance higher than 1000 counts. All peaks determined to be potentially significant for each drug had their  $m/z$  recorded. Unreacted GSH ( $[M-H]^-$   $m/z$  306) was not detected, as the low mass range was set to  $m/z$  400.

The extracted ion chromatogram (XIC) MS spectrum was also collected for each potentially significant peak. The XIC was examined for characteristic fragmentation common to



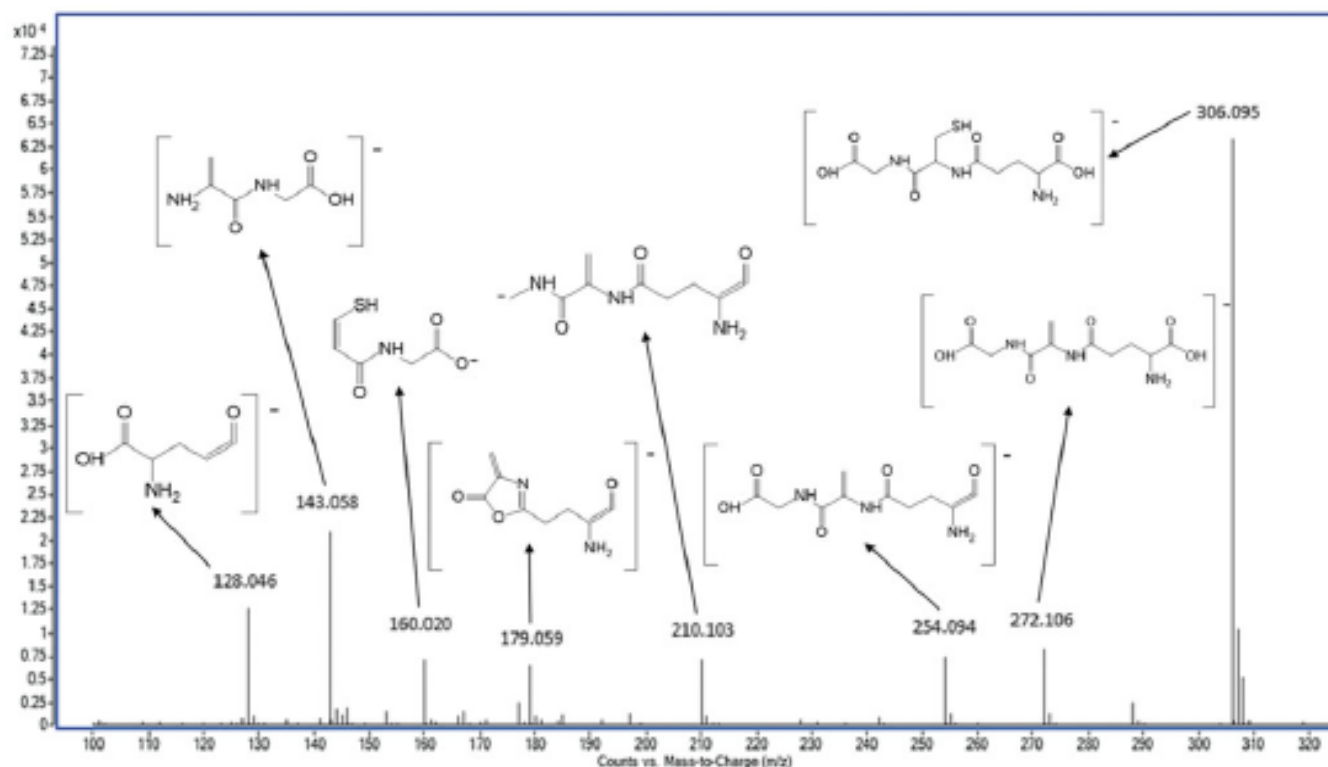


**Figure 2.** LC-QTOF-MS/MS data collected for glutathione. Labelled peaks correspond to a known characteristic GSH ion. Negative ionization structures are provided for each peak.

GSH-containing compounds; since the targeted fragment was a characteristic peak with  $m/z$  of  $[M-H]^- - 272$ , a mass corresponding to the fragment of the adducted compound bound to the GSH sulfur (see Figure 2), additional data needed to be analyzed to confirm presence of GSH. Multiple additional transitions observed in the spectra were also characteristic of GSH;  $m/z$  306, 272, 254, 210, 179, 160, 143 and 128 all agree with published values for GSH analysis in negative mode MS (Dieckhaus et al., 2005).

The software used for data processing and chromatogram peak identification was Agilent (Santa Clara, CA) MassHunter Qualitative Analysis version 8.0. Each peak above the baseline was individually and manually highlighted and analyzed. Once analyzed, the MS fragmentation data were compared to known GSH-containing compound fragmentation patterns (Dieckhaus et al., 2005) to confirm the presence of a GSH adduct. Peaks with matching fragmentation were labeled as prospective ions of interest and were recorded and analyzed further by LC-QTOF-MS. Peaks without corresponding fragmentation were omitted from further analysis, regardless of the results from the initial precursor ion scan.

#### Confirmatory analysis of adduction products via QTOF-MS

Initial analyses by QTOF-MS were performed using full scan mode. In this mode, the mass range was again restricted to  $m/z$  400–800 with fragmentor voltage set to 120 V and no collision induced dissociation. Data were collected for this mass range over the entire run time and any prominent peaks of interest were recorded and then analyzed using targeted MS/MS. In targeted mode, MS/MS data were collected only for the molecular ion peaks of interest, with the mass

range set to  $m/z$  100–800 to allow for smaller identifying fragments to be recorded at collision energies of 10, 20 and 40 eV to allow for full visualization of fragments formed. Compounds with fragmentation consistent with masses commonly seen for fragmentation of GSH were recorded and compared to the list previously compiled from the initial QqQ-MS analyses. In addition, several putative adducts not seen during initial low-resolution MS analysis were observed by QTOF-MS. These putative adducts also exhibited the GSH-characteristic ion with the mass of  $m/z$   $[M-H^+]^- - 272$ . As with the QqQ-MS studies, other ions previously reported to be characteristic of GSH adducts in negative mode ESI were typically present.

#### Identification of adduct structures

Adduct structures were proposed based on accurate mass data for the molecular ion of each drug-GSH adduct and for major MS/MS fragments. Masses consistent with previously reported adducts were assigned the respective structures published in the literature. For novel adducts, a list of metabolites potentially formed *in situ* was compiled using published metabolism data as available and, where not available, manual manipulation of the structure of the parent drug was performed using common metabolic processes found in the literature via ChemDraw Prime software (PerkinElmer, Waltham, MA; version 16.0) until a plausible adduct structure was created. For this purpose, metabolic processes that were examined included hydroxylation (along with NIH shift), O- and N-demethylation, oxidation/reduction, and loss of reactive moieties, as these are common for Phase I metabolic pathways (Schneider & DeCaprio, 2013). Structures associated



with more than one metabolic transformation were also considered. The final theoretical adduct list therefore consisted of multiple target structures for each drug.

Calculated molecular ion masses of the theoretical adduct structures were then compared to those observed in the QTOF-MS/MS analysis for each drug to identify tentative positive hits. For these compounds, MS/MS fragmentation data were then utilized for further confirmation of adduct structure. Both GSH- and drug-specific fragments were considered in this analysis for maximum confidence in the resultant structural assignments. Where present, exact stereo- and regioselectivity of the covalent adduct bond was not identified.

## Results

### Optimization of metabolism/trapping assay system

Optimization of the *in vitro* assay system required numerous factors to be examined. Incubation times of 1, 3, 6 and 12 h were examined, with 3 h determined to be optimal for maximum production of primary metabolites and minimal formation of secondary products. As reported by other investigators (Meyer et al., 2014), glutathione-S-transferase (GST) was included in several trials to determine if its presence would aid in the formation of adducts with GSH. However, there was no observed increase in adduct formation, and GST was therefore eliminated from the protocol for simplicity. The addition of G6P and G6PD provided a regeneration system for NADPH which allowed for optimal enzymatic activity for the duration of the incubation. Initial trials were conducted with a drug: GSH molar ratio of 1:20, however this was later changed to 1:2 (final concentration as stated in Methods) by increasing the concentration of the drug of interest in order to maximize the concentration of the reactive metabolites formed. This ratio is higher than that typically used in metabolic trapping assays. However, while our initial experiments with lower drug concentrations did yield positive results in the QqQ screening procedure, the higher ratio was necessary to produce sufficient product for the QTOF MS/MS analyses.

### QqQ-MS identification of GSH adducts

Figure 3(a) shows an example of a product ion TIC for the positive control drug APAP. A large peak is present at RT 2.6 min; the inset shows numerous additional potentially relevant peaks at lower abundances. XIC analysis of APAP-adducted GSH (Figure 3(b)) revealed one major product at RT 2.68 min with  $m/z$  455 and a minor product at RT 2.36 min with  $m/z$  471. Despite showing counts for the  $m/z$  272 fragment, other peaks in the TIC did not show characteristic GSH fragmentation patterns and were eliminated from further consideration. The APAP-GSH adducts identified in this experiment have been previously reported (Dahlin et al., 1984; Xie et al., 2013).

Using this approach, a total of 20 potentially significant GSH adduction products were identified by LC-QqQ-MS/MS

analysis for 10 of the 16 drugs examined, including APAP, CLZ, COC, DZP, MDMA, MDPV, MOR, NAL, OXY and THC. Multiple adduct structures were also observed for a number of drugs. In contrast, GSH adducts were not observed for ALP, BUP, DZP, META, METH and METY under the conditions used in the study. Target products detected by low resolution MS were then further examined using high resolution LC-QTOF-MS/MS analysis as described below.

### QTOF-MS identification of GSH adducts

Figure 2 shows the high-resolution mass spectrum of GSH, with corresponding fragment structures indicated. Table 2 presents HRMS data (molecular formula, molecular ion and characteristic fragment ions and proposed composition) for all GSH adducts detected in the study, along with literature reference if previously reported. The presence and relative abundance of characteristic GSH fragments (*ie.* "b", "p", "y" and "k" ions) and fragments associated with drug still bound to GSH (*ie.* "d" and "f" ions) provided important data to further elucidate adduct identity and location of the drug-thiol linkage (Xie et al., 2013). In addition, ions associated with fragmentation within the drug moiety itself were occasionally observed. Structural elucidation was facilitated by the generation of fragments at collision energies of 10, 20 and 40 eV (*ie.* top, middle and bottom panels of each adduct MS/MS spectrum in Figures 4 and 5).

As an example of the procedure used to confirm GSH adduct formation and identity based on HRMS data, the molecular ion peak observed at  $m/z$  455.089 for APAP was consistent with a previously reported adduct of the parent drug with GSH (APAP1; Figure 4(a) and Table 2). Major fragment ions for this adduct included the molecular ion ( $m/z$  455.089), five fragments specific to GSH ( $m/z$  272.089, 254.078, 210.088, 143.045, 128.046) (Xie et al., 2013), and a fragment corresponding to the drug moiety bound to the sulfur of GSH ( $m/z$  182.028). A second, less intense molecular ion peak for an acetaminophen-GSH adduct (APAP2) was observed at  $m/z$  471.119, along with three fragments consistent with GSH modification ( $m/z$  272.088, 143.045 and 128.045) in addition to a fragment corresponding to the drug moiety bound to the sulfur of GSH ( $m/z$  198.025) (Figure 4(b) and Table 2). To determine potential structures for this adduct, the parent drug was subjected to manual metabolic modification analysis using ChemDraw Prime software (PerkinElmer, version 16.0) to produce a list of likely alterations occurring from Phase I metabolism. This analysis indicated that hydroxylation of the phenyl ring would produce calculated molecular ion and fragment masses consistent with those observed. This proposed most likely adduct structure has also been previously reported (Xie et al., 2013).

The same general procedure was repeated for all detected putative drug-GSH adducts. Figure 5 shows QTOF MS/MS spectra and proposed structures for all GSH adducts identified in the present study that have not been previously reported in the literature. For dozapine, three GSH adducts were detected. Data for two of these (CLZ1 and CLZ2) are consistent with adducts previously reported by other

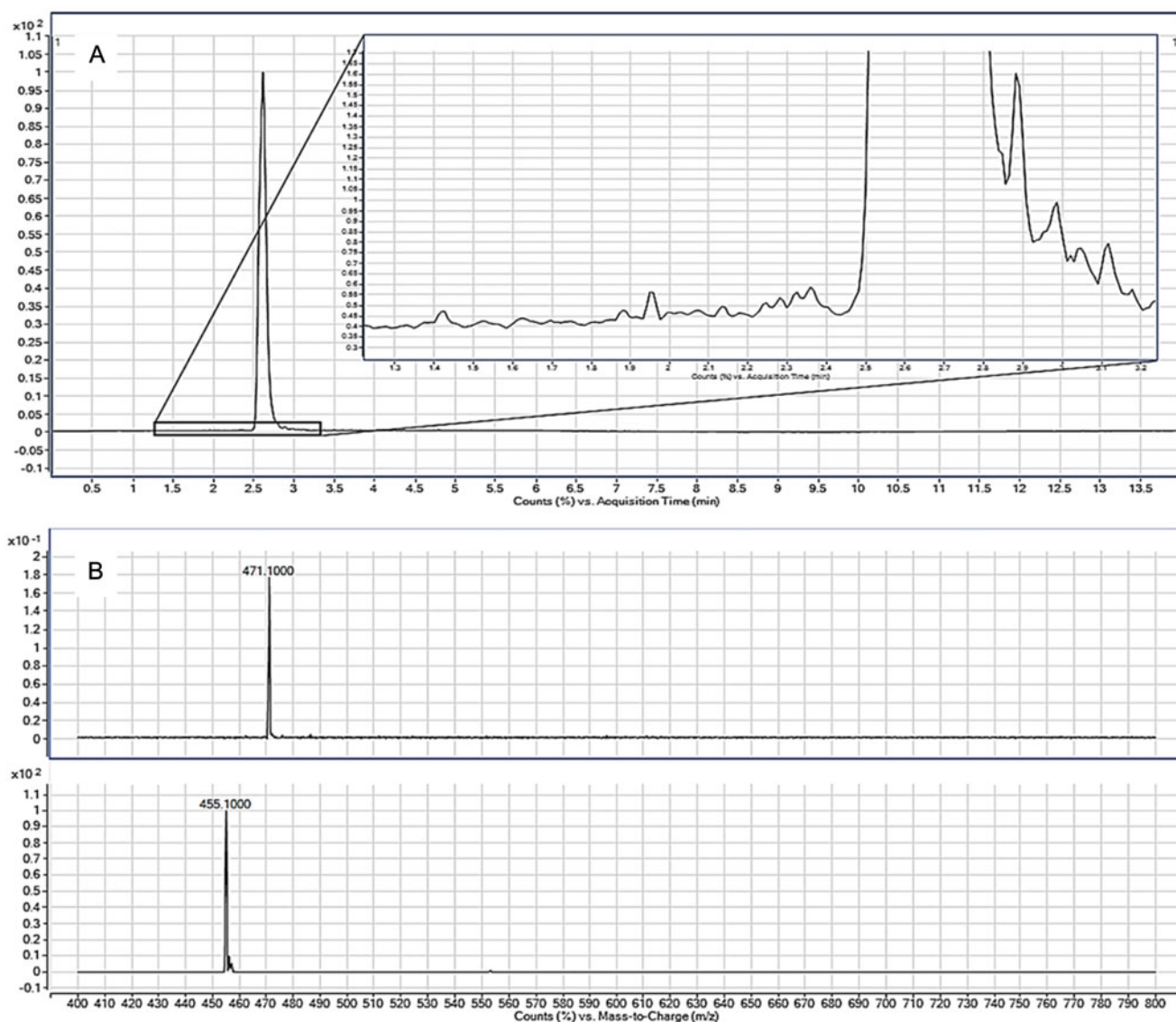


**Figure 3.** (A) TIC of APAP + GSH collected by product ion scan mode via LC-QqQ-MS in negative ionization mode. Inset is zoomed-in portion around the base of the major peak, showing multiple peaks with lesser intensities. (B) XICs for ions at  $m/z$  471 and 455, the two relevant peaks of interest from the TIC.

investigators. In contrast, CLZ3 (Figure 5) represents a novel GSH adduct structure for this drug. For CLZ3, the  $[M-H]^-$  ion with  $m/z$  of 548.099 is consistent with loss of the entire piperazine moiety, in addition to hydroxylation and rearomatization following adduction with GSH. The peak labeled as a “d” transition at  $m/z$  275.005 corresponds to the neutral loss observed from the cleavage of the sulfur of GSH from the rest of the tripeptide. The resulting fragment represents the metabolized CLZ moiety still bound to the sulfur of GSH. The “k” ion corresponds to a characteristic GSH fragment. Rearomatization of the benzene ring is supported by the presence of the “k” peak and lack of an “i” peak, suggesting that conjugation occurs at an aromatic site on the clozapine metabolite (Xie et al., 2013).

DZP1 is a previously unreported adduct for diazepam and was the only one observed for this drug. The presence of the  $[M-H]^-$  ion at  $m/z$  606.154 is consistent with a mechanism involving reduction of the diazepine ketone in the parent drug to a hydroxyl group, hydroxylation of the 5-phenyl

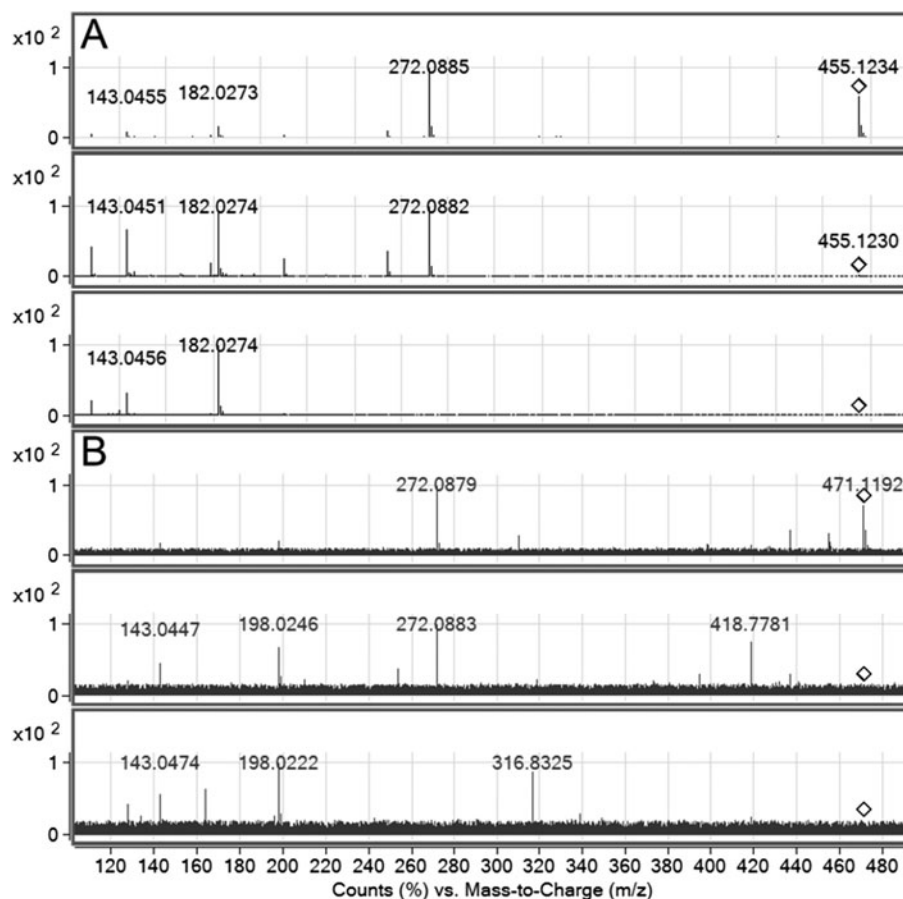
ring and covalent adduction of GSH with rearomatization of the phenyl group. The specific fragment at  $m/z$  588.142 is consistent with cleavage of a hydroxyl group, most likely that attached to the 5-phenyl moiety. The specific fragment at  $m/z$  315.044 may be derived via cleavage of both the 5-phenyl hydroxyl and the phenyl C–S bond of the adduct. Rearomatization of the phenyl ring containing the site of adduction is supported by the presence of the “k” fragment at  $m/z$  272.098 in addition to the lack of an “i” fragment. The remaining “b” and  $m/z$  210.093 ions are each consistent with GSH fragmentation.

MDPV1 is identical in MS/MS characteristics to a previously reported GSH adduct with this compound and which represents adduction to a demethylenated diol metabolite (Meyer et al., 2014). MDPV2 is the first of two previously unreported MDPV adducts observed in this study. The  $[M-H]^-$  ion at  $m/z$  498.172 most likely represents metabolic demethylenation, as with MDPV1, in addition to further metabolic loss of the pyrrolidine ring via *N*-deamination, followed by



**Table 2.** GSH adducts observed for all drugs tested, including proposed formula and composition and major ions.

Drug	Formula	Composition	Ions observed <sup>a</sup>	Reference <sup>b</sup>
APAP1	C <sub>10</sub> H <sub>17</sub> N <sub>3</sub> O <sub>6</sub> S	GSH	306.095, 272.106( <i>k</i> ), 254.094, 210.103, 179.059, 160.020, 143.058( <i>b</i> ), 128.046( <i>f</i> )	Dahlin et al. (1984)
APAP2	C <sub>18</sub> H <sub>24</sub> N <sub>4</sub> O <sub>8</sub> S	D + GSH-2H	455.089, 272.089( <i>k</i> ), 254.078, 210.088, 182.028( <i>d</i> ), 143.045( <i>b</i> ), 128.046( <i>f</i> )	Xie et al. (2013)
CLZ1	C <sub>18</sub> H <sub>24</sub> N <sub>4</sub> O <sub>9</sub> S	D + GSH + O-2H	471.119, 272.088( <i>k</i> ), 198.025 ( <i>d</i> ), 143.045( <i>b</i> ), 128.045( <i>f</i> )	Zhu et al. (2007)
CLZ2	C <sub>28</sub> H <sub>34</sub> CIN <sub>7</sub> O <sub>6</sub> S	D + GSH-2H	630.194, 357.095( <i>d</i> ), 272.089( <i>k</i> ), 254.078, 143.046( <i>b</i> )	Zhu et al. (2007)
CLZ3	C <sub>28</sub> H <sub>36</sub> CIN <sub>7</sub> O <sub>7</sub> S	D + GSH + O	648.198, 272.089( <i>k</i> ), 143.046( <i>b</i> )	na
COC1	C <sub>23</sub> H <sub>24</sub> CIN <sub>5</sub> O <sub>7</sub> S	D + GSH + O-C <sub>5</sub> H <sub>10</sub> N <sub>2</sub>	548.101, 275.005( <i>d</i> ), 272.095( <i>k</i> ), 143.046( <i>b</i> )	Schneider & DeCaprio (2013)
	C <sub>27</sub> H <sub>38</sub> N <sub>4</sub> O <sub>11</sub> S	D + GSH + O	625.230, 565.055, 384.821, 306.080( <i>i</i> ), 272.090( <i>k</i> ), 194.950, 143.046( <i>b</i> )	na
DZP1	C <sub>26</sub> H <sub>30</sub> CIN <sub>5</sub> O <sub>8</sub> S	D + GSH + O	606.154, 588.142, 315.039, 272.088( <i>k</i> ), 258.013, 210.089, 143.046( <i>b</i> )	Meyer et al. (2014)
MDMA1	C <sub>20</sub> H <sub>30</sub> N <sub>4</sub> O <sub>8</sub> S	D + GSH-CH <sub>2</sub>	485.189, 272.090( <i>k</i> ), 212.771( <i>d</i> ), 143.047( <i>b</i> ), 128.045( <i>f</i> )	Meyer et al. (2014)
MDMA2	C <sub>21</sub> H <sub>30</sub> N <sub>4</sub> O <sub>8</sub> S	D + GSH-2H	497.131, 272.091( <i>k</i> ), 254.085, 143.047( <i>b</i> ), 128.046( <i>f</i> )	Meyer et al. (2014)
MDMA3	C <sub>19</sub> H <sub>25</sub> N <sub>3</sub> O <sub>9</sub> S	D + GSH + O-C <sub>2</sub> H <sub>7</sub> N	470.140, 436.793, 272.090( <i>k</i> ), 197.030( <i>d</i> ), 143.046( <i>b</i> ), 128.045( <i>f</i> )	Meyer et al. (2014)
MDPV1	C <sub>25</sub> H <sub>36</sub> N <sub>4</sub> O <sub>9</sub> S	D + GSH-CH <sub>2</sub>	567.238, 294.118( <i>d</i> ), 272.091( <i>k</i> )	Meyer et al. (2014)
MDPV2	C <sub>21</sub> H <sub>29</sub> N <sub>3</sub> O <sub>9</sub> S	D + GSH-C <sub>5</sub> H <sub>8</sub> N	498.172, 272.089( <i>k</i> ), 225.060( <i>d</i> ), 143.046( <i>b</i> ), 139.995	na
MDPV3	C <sub>21</sub> H <sub>29</sub> N <sub>3</sub> O <sub>10</sub> S	D + GSH + O-C <sub>5</sub> H <sub>7</sub> N	514.168, 378.808, 272.103( <i>k</i> ), 241.068( <i>d</i> ), 143.056( <i>b</i> )	na
MOR1	C <sub>27</sub> H <sub>34</sub> N <sub>4</sub> O <sub>9</sub> S	D + GSH-OH	589.219, 316.102( <i>d</i> ), 306.077( <i>i</i> ), 272.089( <i>k</i> ), 210.089, 143.046( <i>b</i> ), 128.045( <i>f</i> )	Todaka et al. (2005)
NAL1	C <sub>30</sub> H <sub>38</sub> N <sub>4</sub> O <sub>10</sub> S	D + GSH-2H	645.249, 306.094( <i>i</i> ), 272.105( <i>k</i> ), 210.089, 143.057( <i>b</i> ), 128.046( <i>f</i> )	na
NAL2	C <sub>30</sub> H <sub>40</sub> N <sub>4</sub> O <sub>11</sub> S	D + GSH + O	663.260, 390.157( <i>d</i> ), 358.184( <i>j</i> ), 306.093( <i>i</i> ), 272.105( <i>k</i> ), 210.089, 143.057( <i>b</i> ), 128.046( <i>f</i> )	na
OXY1	C <sub>28</sub> H <sub>36</sub> N <sub>4</sub> O <sub>10</sub> S	D + GSH-2H	619.208, 408.012, 306.077( <i>i</i> ), 272.958( <i>k</i> ), 210.089, 143.057( <i>b</i> ), 128.046( <i>f</i> )	na
OXY2	C <sub>28</sub> H <sub>34</sub> N <sub>4</sub> O <sub>11</sub> S	D + GSH + O-4H	633.223, 306.076( <i>i</i> ), 272.088( <i>k</i> ), 210.089, 143.057( <i>b</i> ), 128.046( <i>f</i> )	na
THC1	C <sub>31</sub> H <sub>45</sub> N <sub>3</sub> O <sub>9</sub> S	D + GSH + O-2H	634.306, 361.205( <i>d</i> ), 306.095( <i>i</i> ), 272.106( <i>k</i> ), 210.091, 143.058( <i>b</i> ), 128.046( <i>f</i> )	na
THC2	C <sub>31</sub> H <sub>45</sub> N <sub>3</sub> O <sub>10</sub> S	D + GSH + O <sub>2</sub> -2H	650.301, 377.199( <i>d</i> ), 343.193( <i>j</i> ), 306.094( <i>i</i> ), 272.106( <i>k</i> ), 210.091, 143.057( <i>b</i> ), 128.046( <i>f</i> )	na
THC3	C <sub>31</sub> H <sub>45</sub> N <sub>3</sub> O <sub>11</sub> S	D + GSH + O <sub>3</sub> -H	666.297, 393.195( <i>d</i> ), 359.190( <i>j</i> ), 306.094( <i>i</i> ), 272.106( <i>k</i> ), 210.091, 143.057( <i>b</i> ), 128.046( <i>f</i> )	na
THC4	C <sub>31</sub> H <sub>41</sub> N <sub>3</sub> O <sub>12</sub> S	D + GSH + O <sub>4</sub> -4H	678.304, 306.095( <i>i</i> ), 272.106( <i>k</i> ), 210.091, 143.058( <i>b</i> ), 128.046( <i>f</i> )	na

<sup>a</sup>Molecular ion in bold; letters in parentheses refer to characteristic GSH fragments according to nomenclature of Xie et al. (2013).<sup>b</sup>Literature reference for previously reported adduct; na – not previously reported.**Figure 4.** LC-QTOF-MS/MS spectra for the two GSH adduct peaks of interest observed for APAP; (A) *m/z* 455.089 and (B) *m/z* 471.119. The top, middle, and bottom panel for each spectrum represents collision energies of 10, 20 and 40 eV, respectively. The use of multiple collision energies allowed for optimum generation of identifying fragments.

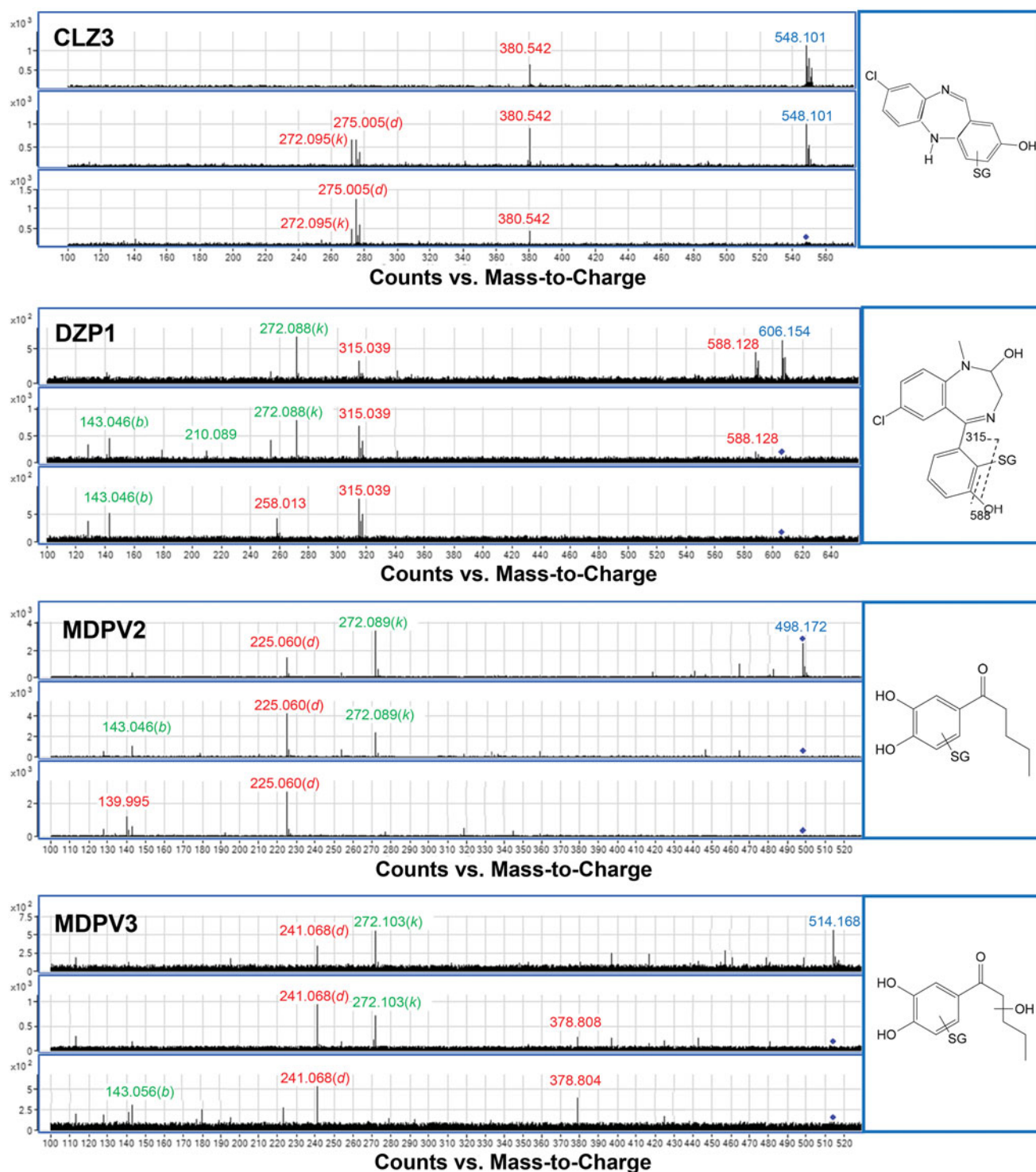


**Figure 5.** MS/MS spectra for all 12 previously unreported adducts. In online version, the molecular ion is represented in blue, GSH-specific peaks in green, and structurally significant peaks for GSH-containing compounds in red. Letters in italics refer to characteristic GSH derived fragments. Proposed structures for 9 of the 12 adducts are also shown with GSH linkage indicated.

covalent adduction by the GSH thiol on the phenolic ring. The presence of a “*d*” fragment at  $m/z$  225.060 further supports the identity of the adducted drug moiety, as it corresponds to the mass of the moiety plus the sulfur of GSH. The presence of a “*k*” fragment with  $m/z$  272.089 and lack of a detectable “*i*” fragment strongly indicates linkage of the GSH sulfur to an aromatic carbon. The remaining “*b*” ion at  $m/z$  143.046 represents a GSH fragment.

MDPV3 is a second unreported GSH adduct for this compound. Similar to MDPV2, the  $[M-H]^-$  ion at  $m/z$  514.168 is consistent with demethylation, loss of the pyrrolidine ring and covalent adduction of the GSH thiol. However, the precursor ion mass for MDPV3 also indicates addition of a hydroxyl group, most likely on the alkyl chain moiety. This interpretation is corroborated by the presence of a “*d*” ion with  $m/z$  241.068. Again, the presence of a “*k*” fragment at

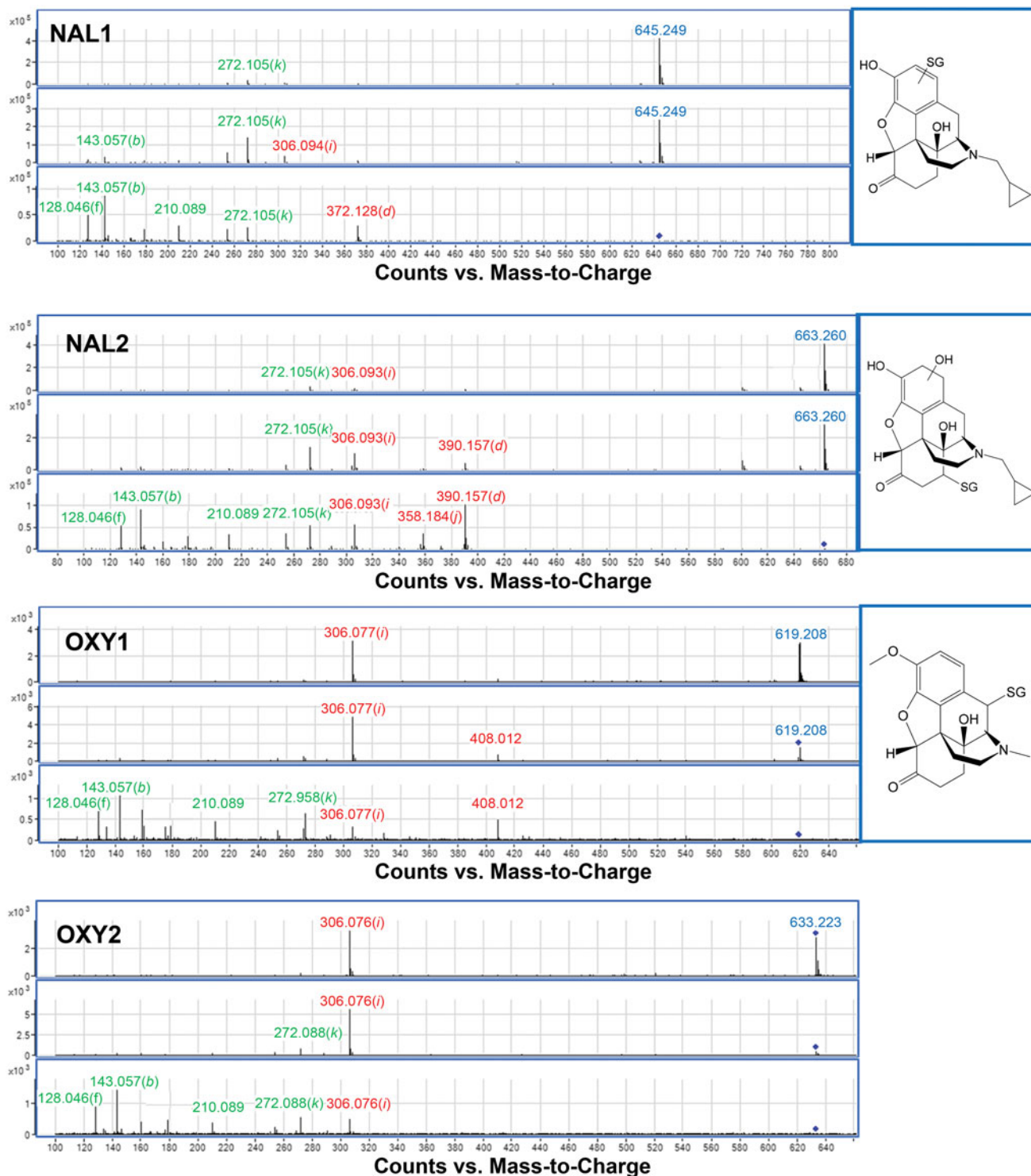


Figure 5. Continued.

$m/z$  272.103 along with the lack of an "i" fragment supports an aromatic thiol linkage. The remaining "b" ion represents a GSH fragment, while the ion at  $m/z$  378.808 is unidentified.

Two naltrexone-GSH adducts were observed in the present study and are the first such derivatives reported in the literature. For NAL1, a  $[M-H]^-$  ion at  $m/z$  645.249 is consistent with unmodified precursor drug directly adducted to GSH. The MS/MS spectrum clearly shows the presence of "k" ions with lower intensities of "i" and "d" ions (Figure 5). While not

unequivocal, this pattern is most consistent with thiol conjugation to the benzene ring in naltrexone. The "p" and "b" ions represent GSH fragments.

The MS/MS spectrum for NAL2 exhibits an  $[M-H]^-$  ion at  $m/z$  663.260, which is most consistent with GSH conjugation to a hydroxylated metabolite. This interpretation is also supported by the presence of a "d" fragment at  $m/z$  390.157 and a "j" fragment at  $m/z$  358.184. The similar relative abundances of the "k" and "i" ions along with the higher



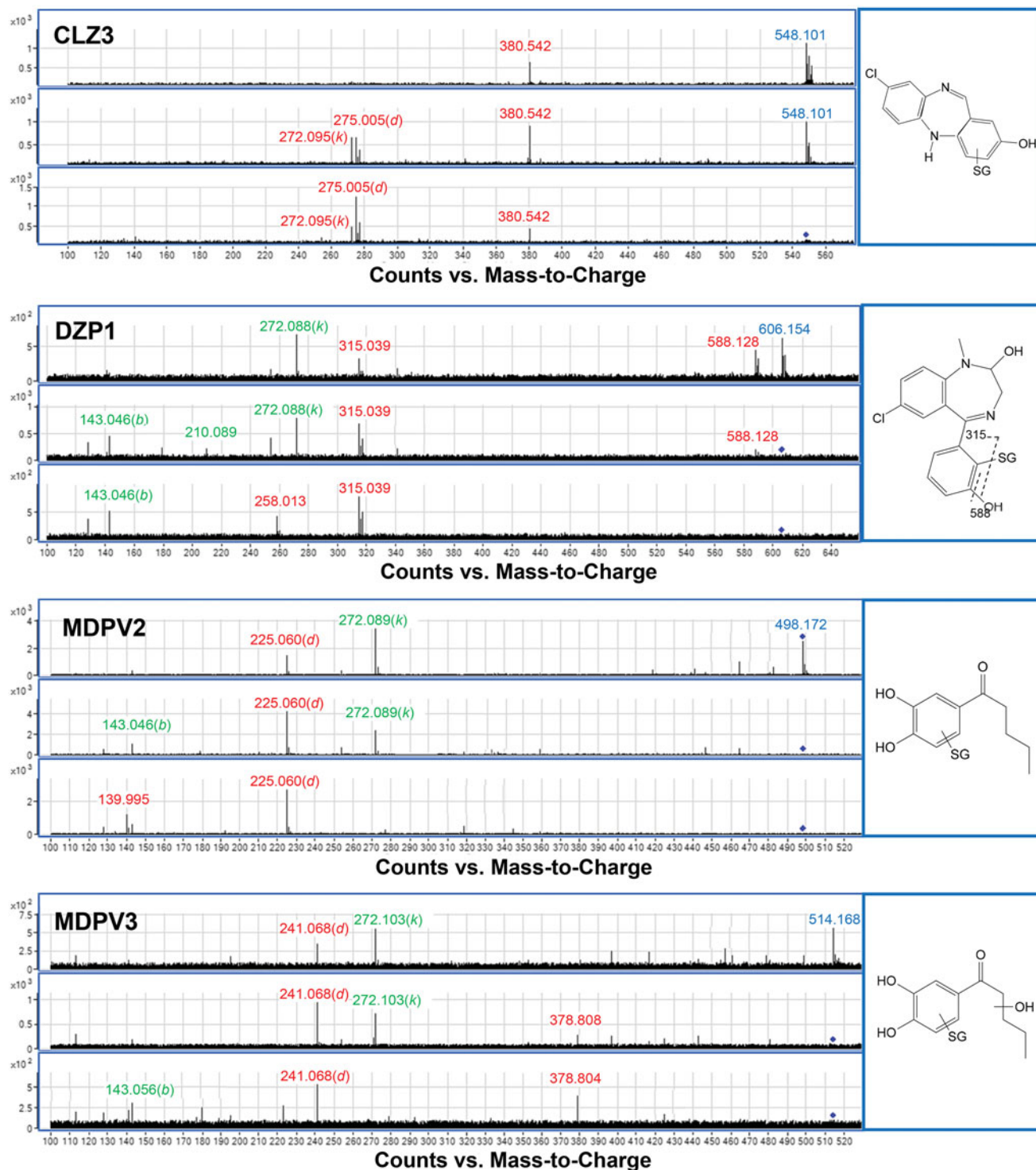


Figure 5. Continued.

abundance of "d" as compared to "j" ions suggest linkage of the thiol sulfur of GSH to an aliphatic carbon in the drug moiety (Xie et al., 2013). While Figure 5 shows one possible structure consistent with these data, the position of the hydroxyl group and C-S link cannot be unequivocally determined without additional information.

GSH adducts with oxycodone have not previously been reported. In the present study, OXY1 exhibited a  $[M-H]^-$  ion at  $m/z$  619.208, consistent with GSH adduction to parent

drug. The presence of an "i" fragment at  $m/z$  306.077 at a much higher abundance than the "k" ion at  $m/z$  272.958, along with the absence of a "d" ion, is strongly suggestive of a GSH thiol linkage to a benzylic carbon. The determination of a benzylic linkage is in agreement with the literature on GSH adduct linkage sites (Xie et al., 2013). Based on these data, a possible structure for the OXY1 adduct is shown in Figure 5. Evidence for a second GSH-oxycodone adduct (OXY2) was also obtained. The  $[M-H]^-$  ion at  $m/z$  633.223 is

14 Da larger than the OXY1 species, suggesting GSH adduction to a metabolite of the drug. As with OXY1, the presence of a high abundance “i” fragment at  $m/z$  306.077 combined with the lack of a “d” ion is strongly suggestive of a GSH thiol linkage to a benzylic carbon. However, without additional data, a putative structure for this adduct is not proposed.

GSH adducts of  $\Delta^9$ -tetrahydrocannabinol (THC) have not previously been reported in the literature. The present study identified four species consistent with covalent adduction of GSH with THC, all proposed to result from modification of THC metabolites oxidized at the 11 position or on the pentyl chain of the parent drug. THC1 exhibited a  $[M-H]^-$  ion at  $m/z$  634.306, consistent with GSH adduction to 11-hydroxy- $\Delta^9$ -THC, a prominent metabolite of this cannabinoid (Dinis-Oliveira, 2016). The presence of a major “d” ion at  $m/z$  361.205 in addition to the “i” fragment further supports this interpretation. The data most support a benzylic C–S linkage between the drug moiety and GSH, based on the substantially higher intensity of the “i” fragment as compared to that of the “k” ion (Figure 5). However, due to the presence of a definite “d” fragment, an aliphatic linkage cannot be entirely ruled out.

The THC2 moiety exhibited a  $[M-H]^-$  ion at  $m/z$  650.301, which is consistent with conjugation of GSH with another common THC metabolite, *i.e.* 11-nor-9-carboxy- $\Delta^9$ -THC. This interpretation is also supported by the presence of a “d” fragment at  $m/z$  377.199. The covalent linkage between the drug moiety and the GSH sulfur is most likely aliphatic, since the intensity of the “k” ion (at  $m/z$  272.106) is higher than that of the “i” fragment at  $m/z$  306.094.

The structures of the detected adducts represented by THC3 and THC4 are more speculative, as they appear to involve adduction of secondary oxidized THC metabolites. For example, THC3 exhibited a  $[M-H]^-$  ion at  $m/z$  666.297, which would be consistent with GSH adduction to a hydroxylated metabolite of 11-nor-9-carboxy- $\Delta^9$ -THC, a conclusion further supported by the presence of the drug-specific “d” fragment at  $m/z$  393.195. The lack of prominent “i” ions in the spectrum suggests linkage of aromatic carbon to the GSH sulfur. The MS/MS spectrum of THC4 exhibited a  $[M-H]^-$  ion at  $m/z$  678.334, *i.e.* 38 Da higher than observed for THC2. This observation would be consistent with GSH adduction to a metabolite of 11-nor-9-carboxy- $\Delta^9$ -THC containing a second carboxyl function. Furthermore, the appearance of “i” ions at much higher intensity than “k” ions, in addition to the absence of “d” ions in this spectrum, suggests a linkage of the GSH sulfur to a benzylic carbon. Nevertheless, additional data are required to identify the exact nature of the metabolic modifications present in the THC3 and THC4 adducts and the location of the C–S linkage in each species.

## Discussion

This research explored the capability of selected drugs of abuse to form adducts with the tripeptide glutathione. The formed adducts result from covalent bonds between the

nucleophilic sulfur in GSH and an electrophilic site on the parent drug or a metabolite. The formation of GSH-based adducts with drugs of abuse has only been sparingly reported in the literature, with available data limited to cocaine (Schneider & DeCaprio, 2013), MDMA and MDPV (Meyer et al., 2014), and morphine (Todaka et al., 2005). In these examples, MDMA was the only compound with reported GSH adducts formed by both the precursor drug and a metabolite. While previous work with these drugs has demonstrated the capability to form adducts with GSH, there is clearly a lack of available information on this phenomenon for other widely abused substances.

Of the 22 GSH adducts observed in this study, nine have been previously reported in the literature (see Table 2 for references). The structures reported previously have masses which match closely with those observed in spectra collected in the present study (Dahlin et al., 1984; Meyer et al., 2014; Schneider & DeCaprio, 2013; Todaka et al., 2005; Zhu et al., 2007). A direct comparison of our spectral data with previous reports is possible for MDMA and MDPV, where negative mode MS ionization and analysis was also utilized. MS/MS data for fragments of GSH and GSH containing compounds and molecular ion exact masses observed for MDMA1, MDMA2, MDMA3 and MDPV1 in the present study agree with the data previously reported with negative mode analysis (Meyer et al., 2014).

Manual metabolite prediction analysis suggested that, in many cases, formation of the adduct is associated with an “NIH shift” pathway. There are several proposed mechanisms by which an NIH shift may occur, however, the prevailing theory, which has been experimentally corroborated, involves formation of an unstable epoxide which then undergoes a hydride shift (Jerina & Daly, 1974; Ortiz de Montellano & Nelson, 2011). While this process is typically followed by a rearomatization step, in situations where GSH or a similar nucleophile is present, rearomatization is not always seen (Guengerich, 2003).

Plausible structures are proposed for the majority of the previously unreported adducts identified in the present study, based upon HRMS accurate mass and MS/MS data and likely metabolic transformations. However, for the OXY2, THC3 and THC4 adducts, the available data were insufficient to propose a structure with a high degree of confidence. The fragmentation patterns suggest that both OXY2 and THC4 have benzylic covalent thiol linkages, while THC3 likely contains an aromatic linkage. The molecular ion masses of THC3 and THC4 seem to suggest further metabolic modifications to the metabolite 11-nor-9-carboxy- $\Delta^9$ -THC prior to covalent adduction with GSH, such as a hydroxylation or further carbonylation. OXY2 also appears to have undergone additional metabolic modification prior to adduction, although the exact steps are unclear.

While NAL1 and OXY1 have an adduct mass which corresponds to the parent drug directly bound to GSH without any other modifications, the other structures proposed for GSH adducts in Table 2 represent adducts formed by one or more primary metabolites of the drug. One of the initial metabolic steps is likely to be hydroxylation, as is consistent



with the proposed structures for CLZ1, DZP1, MDPV3 and NAL2. Hydroxylations are common oxidative steps in the metabolic pathways of CLZ, DZP and MDPV, although this pathway has not been reported for NAL (de Almeida et al., 2015; Schaber et al., 1998; Yamada et al., 2005).

Structures consistent with bond cleavage within the drug moiety were also observed for three of the adducts. CLZ3 is proposed to have lost the piperazine ring in addition to undergoing hydroxylation and rearomatization. While this particular metabolite has not previously been reported in the literature, there have been observations of modifications to the piperazine ring in CLZ, indicating that it may be a site of potential metabolic processes resulting in loss of piperazine ring (Dragovic et al., 2013). Loss of a piperazine ring has been exhibited in the metabolism of other heterocycle containing compounds such as aildenafil (Li et al., 2014).

Formation of MDPV2 is associated with loss of the methylene bridge and pyrrolidine moiety (via oxidative deamination) in addition to rearomatization, while MDPV3 may form via the same process in addition to a hydroxylation on the resultant alkyl chain. Demethylenation, common to either the orthocatechol or orthoquinone, and oxidative deamination of methylenedioxy type drugs has been reported in the literature (Meyer & Maurer, 2010; Yamada et al., 2005). The orthoquinone formed by some methylenedioxy drugs has been reported to be the reactive metabolite responsible for toxicity (Kalgutkar et al., 2005). As mentioned previously, some of the drugs underwent a rearomatization step following GSH adduction and NIH shift (CLZ1, MDPV1, MDPV2, NAL1, OXY1, THC1 and THC2) while others did not (DZP1 and NAL2). This observation is similar to what has been generally reported in the literature involving NIH shifts (Guengerich, 2003).

GSH adducts with  $\Delta^9$ -THC have not been previously reported. The proposed structures for THC1 and THC2 are consistent with adducts formed from the stable metabolites 11-OH- $\Delta^9$ -THC and 11-nor-9-carboxy- $\Delta^9$ -THC, respectively, with direct binding to GSH. The fragmentation patterns and peak ratios discussed in the Results section indicate the thiol linkages appear to be benzylic for THC1 and aliphatic for THC2. The fact that these adducts are consistent with the stable metabolites implies that there may be a reactive intermediate formed, allowing for electrophilic interactions with the thiol moiety from GSH.

For the MS analysis of the GSH compounds in the present study, negative mode scanning was utilized. This was chosen primarily to facilitate analysis of adducted GSH fragmentation. GSH fragmentation patterns in negative mode are well-established in the literature, and in fact have been studied for a variety of covalent adducts, including those with aromatic, aliphatic and benzylic linkages (Dieckhaus et al., 2005; Xie et al., 2013). The observed transitions also provided more prominent and clearer ion signals than those following initial analyses utilizing positive mode scanning. Additionally, many of the parent drugs included here do not produce prominent molecular ions or fragment ions in negative mode, thus minimizing potential interferences due to coelution with unreacted drug present in the assay mixture at significantly higher concentrations than the formed adducts.

While positive mode analysis of the novel GSH adducts could provide additional data for structural confirmation, preliminary use of positive mode for several of the drugs in the present study did not provide useful fragmentation data. As other authors have reported, positive mode ionization is not always helpful for characterization of GSH adducts, particularly with certain drugs where doubly charged  $[M + 2H]^+$  ions are formed, as these do not allow for the neutral loss analysis which is generally utilized in positive mode GSH studies (Dieckhaus et al., 2005). Although negative ionization mode alone did not provide the data necessary for complete structural analysis of all adducts, this approach did provide sufficient information to determine a plausible adduct structure for most of the drugs under study. Unequivocal structural confirmation, including identification of regioselectivity of adduct formation where present, will require additional work with synthetic standards and further analysis by HRMS and definitive techniques such as NMR.

The present work utilized *in vitro* reactive metabolite trapping assays to generate adducts of GSH and a number of common drugs of abuse. The ability of many of these compounds and metabolites to bind to GSH has implications for both toxic mechanisms of action and approaches to longer-term exposure biomonitoring for these drugs. The data also suggest that many of these drugs have the potential to bind to protein thiols *in vivo*. This phenomenon may have important implications for longer-term biomonitoring of abused drugs, where analysis of such adducted protein could be usefully applied in areas of drug testing and forensic toxicological analysis. At the present time, hair analysis is the only available method for long-term detection of illicit drug use. However, hair analysis suffers from methodological and interpretive challenges, and the mechanisms by which most drugs incorporate into hair are not clearly established (Wennig, 2000). Current work in this laboratory is focused on assessing thiol modification in human proteins by reactive metabolites of abused drugs and developing technology for routine monitoring of such modifications as an alternative to hair analysis.

## Disclosure statement

No potential conflict of interest was reported by the authors.

## Funding

This project was supported by Award No. 2015-NE-BX-K001 (to APD), awarded by the National Institute of Justice, Office of Justice Programs, U.S. Department of Justice. The opinions, findings, and conclusions or recommendations are those of the authors and do not necessarily reflect those of the Department of Justice.

## References

- Attia SM. (2010). Deleterious effects of reactive metabolites. *Oxid Med Cell Longev* 3:238–53.
- Blair IA. (2010). Analysis of endogenous glutathione-adducts and their metabolites. *Biomed Chromatogr* 24:29–38.
- Capela JP, Macedo C, Branco PS, et al. (2007). Neurotoxicity mechanisms of thioether ecstasy metabolites. *Neuroscience* 146:1743–57.

- Dahlin DC, Miwa GT, Lu AY, Nelson SD. (1984). N-acetyl-p-benzoquinone imine: a cytochrome P-450-mediated oxidation product of acetaminophen. *Proc Natl Acad Sci USA* 81:1327–31.
- de Almeida CAA, Oliveira MS, Mallmann CA, Martins AF. (2015). Determination of the psychoactive drugs carbamazepine and diazepam in hospital effluent and identification of their metabolites. *Environ Sci Pollution Res* 22:17192–201.
- DeCaprio AP. (1997). Biomarkers: coming of age for environmental health and risk assessment. *Environ Sci Technol* 31:1837–48.
- Dieckhaus CM, Fernandez-Metzler CL, King R, et al. (2005). Negative ion tandem mass spectrometry for the detection of glutathione conjugates. *Chem Res Toxicol* 18:630–8.
- Dinis-Oliveira RJ. (2016). Metabolomics of  $\Delta$ 9-tetrahydrocannabinol: implications in toxicity. *Drug Metab Rev* 48:80–7.
- Dragovic S, Gunness P, Ingelman-Sundberg M, et al. (2013). Characterization of human cytochrome P450s involved in the bioactivation of clozapine. *Drug Metab Dispos* 41:651–8.
- Evans DC, Watt AP, Nicoll-Griffith DA, Baillie TA. (2004). Drug-protein adducts: an industry perspective on minimizing the potential for drug bioactivation in drug discovery and development. *Chem Res Toxicol* 17:3–16.
- Gomez-Lechon MJ, Tolosa L, Donato MT. (2016). Metabolic activation and drug-induced liver injury: in vitro approaches for the safety risk assessment of new drugs. *J Appl Toxicol* 36:752–68.
- Guengerich FP. (2003). Cytochrome P450 oxidations in the generation of reactive electrophiles: epoxidation and related reactions. *Arch Biochem Biophys* 409:59–71.
- Ikehata K, Duzhak TG, Galeva NA, et al. (2008). Protein targets of reactive metabolites of thiobenzamide in rat liver *in vivo*. *Chem Res Toxicol* 21:1432–42.
- Inoue K, Shibata Y, Takahashi H, et al. (2009). A trapping method for semi-quantitative assessment of reactive metabolite formation using [ $^{35}$ S]cysteine and [ $^{14}$ C]cyanide. *Drug Metab Pharmacokinet* 24:245–54.
- Jerina DM, Daly JW. (1974). Arene oxides: a new aspect of drug metabolism. *Science* 185:573–82.
- Kalgutkar AS. (2011). Handling reactive metabolite positives in drug discovery: what has retrospective structure-toxicity analyses taught us?. *Chem Biol Interact* 192:46–55.
- Kalgutkar AS, Gardner I, Obach RS, et al. (2005). A comprehensive listing of bioactivation pathways of organic functional groups. *Curr Drug Metab* 6:161–225.
- Kovacic P, Cooksy AL. (2005). Unifying mechanism for toxicity and addiction by abused drugs: electron transfer and reactive oxygen species. *Med Hypoth* 64:357–66.
- Li Y, Wu L, Gu Y, et al. (2014). Metabolism of aildenafil *in vivo* in rats and *in vitro* in mouse, rat, dog, and human liver microsomes. *Drug Test Anal* 6:552–62.
- Lu D, Sullivan MM, Phillips MB, Peterson LA. (2009). Degraded protein adducts of cis-2-butene-1,4-dial are urinary and hepatocyte metabolites of furan. *Chem Res Toxicol* 22:997–1007.
- Meneses-Lorente G, Sakatis MZ, Schulz-Utermoehl T, et al. (2006). A quantitative high-throughput trapping assay as a measurement of potential for bioactivation. *Anal Biochem* 351:266–72.
- Meyer MR, Maurer HH. (2010). Metabolism of designer drugs of abuse: an updated review. *Curr Drug Metab* 11:468–82.
- Meyer MR, Richter LHJ, Maurer HH. (2014). Methylendioxy designer drugs: mass spectrometric characterization of their glutathione conjugates by means of liquid chromatography-high-resolution mass spectrometry/mass spectrometry and studies on their glutathionyl transferase inhibition potency. *Anal Chim Acta* 822:37–50.
- Miller JA, Miller EC. (1965). Metabolism of drugs in relation of carcinogenicity. *Ann N Y Acad Sci* 123:125–40.
- Ndikum-Moffor FM, Munson JW, Bokinkere NK, et al. (1998). Immunochemical detection of hepatic cocaine-protein adducts in mice. *Chem Res Toxicol* 11:185–92.
- Ortiz de Montellano PR, Nelson SD. (2011). Rearrangement reactions catalyzed by cytochrome P450s. *Arch Biochem Biophys* 507:95–110.
- Schaber G, Stevens I, Gaertner HJ, et al. (1998). Pharmacokinetics of clozapine and its metabolites in psychiatric patients: plasma protein binding and renal clearance. *Br J Clin Pharmacol* 46:453–9.
- Schadt S, Simon S, Kustermann S, et al. (2015). Minimizing DILI risk in drug discovery - A screening tool for drug candidates. *Toxicol in Vitro* 30:429–37.
- Schneider KJ, DeCaprio AP. (2013). Covalent thiol adducts arising from reactive intermediates of cocaine biotransformation. *Chem Res Toxicol* 26:1755–64.
- Shimizu E, Hashimoto K, Komatsu N, Iyo M. (2002). Roles of endogenous glutathione levels on 6-hydroxydopamine-induced apoptotic neuronal cell death in human neuroblastoma SK-N-SH cells. *Neuropharmacol* 43:434–43.
- Thompson RA, Isin EM, Li Y, et al. (2011). Risk assessment and mitigation strategies for reactive metabolites in drug discovery and development. *Chem Biol Interact* 192:65–71.
- Todaka T, Ishida T, Kita H, et al. (2005). Bioactivation of morphine in human liver: isolation and identification of morphinone, a toxic metabolite. *Biol Pharm Bull* 28:1275–80.
- Wennig R. (2000). Potential problems with the interpretation of hair analysis results. *Forensic Sci Int* 107:5–12.
- Xie C, Zhong D, Chen X. (2013). A fragmentation-based method for the differentiation of glutathione conjugates by high-resolution mass spectrometry with electrospray ionization. *Anal Chim Acta* 788:89–98.
- Yamada H, Ishii Y, Oguri K. (2005). Metabolism of drugs of abuse: its contribution to the toxicity and the inter-individual differences in drug sensitivity. *J Health Sci* 51:1–7.
- Yamaoka T, Kitamura Y. (2015). Characterization of a highly sensitive and selective novel trapping reagent, stable isotope labeled glutathione ethyl ester, for the detection of reactive metabolites. *J Pharmacol Toxicol Meth* 76:83–95.
- Zhu M, Ma L, Zhang H, Humphreys WG. (2007). Detection and structural characterization of glutathione-trapped reactive metabolites using liquid chromatography-high-resolution mass spectrometry and mass defect filtering. *Anal Chem* 79:8333–41.